NASA TECHNICAL NOTE

NASA TN D-7138

NASA TN D-7138

PRESSURES AND TEMPERATURES ON THE LOWER SURFACES OF AN EXTERNALLY BLOWN FLAP SYSTEM DURING FULL-SCALE GROUND TESTS

by Donald L. Hughes

Flight Research Center
Edwards, Calif. 93523

NATIONAL AERONAUTICS AND SPACE ADMINISTRATION • WASHINGTON, D. C. • JANUARY 1973

1. Report No.	2. Government Accession No.	3. Recipient's Catalog No.
NASA TN D-7138		

4. Title and Subtitle	5. Report Date
PRESSURES AND TEMPERATURES ON THE LOWER SURFACES OF AN EXTERNALLY BLOWN FLAP SYSTEM DURING FULL-SCALE GROUND TESTS	January 1973
	6. Performing Organization Code
7. Author(s)	8. Performing Organization Report No.
Donald L. Hughes	H-729
	10. Work Unit No.
9. Performing Organization Name and Address	741-72-09-00-24
NASA Flight Research Center P. O. Box 273 Edwards, California 93523	11. Contract or Grant No.
	13. Type of Report and Period Covered
12. Sponsoring Agency Name and Address	Technical Note
National Aeronautics and Space Administration Washington, D. C. 20546	14. Sponsoring Agency Code

15. Supplementary Notes

16. Abstract

Full-scale ground tests of an externally blown flap system were made using the wing of an F-111B airplane and a CF700 engine. Pressure and temperature distributions were determined on the undersurface of the wing, vane, and flap for two engine exhaust nozzles (conical and daisy) at several engine power levels and engine/wing positions. The tests were made with no airflow over the wing. The wing sweep angle was fixed at 26°; the angle of incidence between the engine and the wing was fixed at 3°; and the flap was in the retracted, deflected 35°, and deflected 60° positions. The pressure load obtained by integrating the local pressures on the undersurface of the flap, F_p, was approximately three times greater at the 60° flap position than at the 35° flap position. At the 60° flap position, F_p was between 40 percent and 55 percent of the engine thrust over the measured range of thrust. More than 90 percent of F_p was contained within ±20 percent of the flap span centered around the engine exhaust centerline with both nozzle configurations. Maximum temperatures recorded on the flaps were 218° C (424° F) and 180° C (356° F) for the conical and daisy nozzles, respectively.

17. Key Words (Suggested by Author(s))	18. Distribution Statement
Externally blown flap Undersurface pressures and temperatures	Unclassified - Unlimited

19. Security Classif. (of this report)	20. Security Classif. (of this page)	21. No. of Pages	22. Price*
Unclassified	Unclassified	32	$3.00

* For sale by the National Technical Information Service, Springfield, Virginia 22151

PRESSURES AND TEMPERATURES ON THE LOWER SURFACES OF AN EXTERNALLY BLOWN FLAP SYSTEM DURING FULL-SCALE GROUND TESTS

Donald L. Hughes
Flight Research Center

INTRODUCTION

The need for a commercial air transport which is economically sound and which can operate out of conveniently located airports with short landing strips is widely recognized. The Government is taking steps to help develop a short-takeoff-and-landing (STOL) airplane which would meet these requirements. To achieve short takeoff and landing distances without sacrificing the high wing loading needed for passenger ride comfort or the ability to maintain high cruise speeds, an augmented lift device must be used.

Augmented lift is used in an externally blown flap system which is being considered for use on an experimental NASA STOL airplane. In this system the primary thrust engines are close to the undersurface of the wing, so that when the flaps are lowered the jet exhaust impinges on the flap. Additional lift results from increased circulation about the wing and from the momentum change of the deflected jet stream.

A survey of the areas of engine exhaust flow impingement on the flap and wing of an externally blown flap system is needed to determine the spanwise pressure distribution as well as the actual flap loads and temperatures generated. Although some attempts to obtain pressure distributions on a wing and flap system have been made by using scale models in wind tunnels, little has been done with full-scale wings and engines in an environment free of wind-tunnel interference effects. Thus the NASA Flight Research Center installed pressure and temperature instrumentation on the wing of an F-111B airplane. This wing, which has a double-slotted flap, was mounted vertically on a test stand adjacent to a CF700 turbofan engine (fig. 1) with an extended tailpipe. The engine was positioned so that the jet exhaust impinged on the flap when extended. Tests were made with no airflow over the wing other than that induced by the engine jet. The position of the wing with respect to the engine could be varied, and the wing sweep, angle of incidence between the engine and the wing, and flap positions could also be changed.

This report presents wing surface pressure and temperature data obtained during the ground tests with the leading-edge wing sweep fixed at 26° and the angle of incidence between the engine and wing fixed at 3°. Surface pressures recorded during tests in which a conical and a daisy engine exit nozzle were used with various engine power

levels, flap deflections, and relative engine/wing positions are compared. High response pressure transducer data were also measured on the flap surface.

SYMBOLS

Physical quantities in this report are given in the International System of Units (SI) and parenthetically in U.S. Customary Units. The measurements were taken in Customary Units. Factors relating the two systems are presented in "The International System of Units - Physical Constants and Conversion Factors" (NASA SP-7012) by E. A. Mechtly.

F_m	measured engine thrust at 701 meters (2300 feet) altitude, N (lbf)
F_p	pressure load obtained by integration of local pressures on undersurface of flap or vane, N (lbf)
$\frac{N_f}{\sqrt{\theta}}$	fan rotor speed corrected to standard day sea-level temperature, rpm or rps
p	local pressure, N/m^2 (lbf/in^2)
p_o	ambient static pressure, N/m^2 (lbf/in^2)
T	temperature, °C (°F)
T_o	ambient temperature, °C (°F)
x	distance along engine centerline from nozzle face to flap surface (fig. 5), m (in.)
y	distance from centerline of engine exhaust at nozzle face to wing surface, m (in.)
ω	angle of incidence between engine and wing
Subscripts:	
a, b, c	nozzle locations relative to flap surface that were determined with the engine at y_e and flaps at 60° (fig. 5)
d, e, f	nozzle locations relative to wing
u, v, w	high response static pressure measuring locations on flap

DESCRIPTION OF APPARATUS

Test Configuration

Wing. – The inboard half of an F-111B left wing was mounted vertically on a movable platform installed on an engine runup ramp at Edwards Air Force Base, Calif. The position of the wing with respect to the engine exhaust nozzle could be varied in several ways: distance from the flap (longitudinally); closeness to the wing (laterally); angle of incidence between the engine and wing; and angle of leading-edge sweep. All the test data presented were obtained with the flaps in three positions: retracted, extended and deflected 35°, and extended and deflected 60°. (The flap positions are referred to as retracted, 35°, and 60°.) The 60° position was not a normal flap position on the F-111B wing; thus the flaps were held in a special support fixture mounted on the upper surface of the wing and flap at the normal flap rail locations. Figures 2(a) to 2(c) show the undersurface of the wing with the flaps in the three positions. A cross section of the aerodynamically shaped vane, which was positioned between the wing and the flap, is shown in figure 3. The term "double-slotted flap" was derived from the two gaps between the flap and vane, and the vane and wing. The test results presented were obtained with the wing sweep angle set at 16° at the 60-percent wing chord (rear spar), which resulted in a leading edge sweep of approximately 26°. No pressure or flow measurements were made on the upper surface of the wing, vane, or flap.

Engine. – A General Electric CF700 turbofan engine was mounted in a fixed position on the thrust stand adjacent to the wing (fig. 1). A bellmouth inlet and an acoustically treated exhaust duct which terminated in one of two interchangeable exit nozzles were connected to the engine. A closeup photograph of the conical exit nozzle is shown in figure 4(a), and a photo of a General Electric CJ805 daisy nozzle is shown in figure 4(b). The conical nozzle had approximately the same exhaust exit area as the daisy nozzle.

Wing/engine relationships. – The wing, flap, and nozzle positions and their relationships are shown in figure 5. All the test data were obtained with an angle of incidence between the engine and wing of approximately 3°. The longitudinal nozzle positions (x-dimensions) were determined as an approximate multiple of conical nozzle diameters along the y_e centerline to the point of jet impingement on the 60° flap position. Therefore, the x_a position was established at approximately 3 diameters from the point of centerline jet impingement on the 60° flap position, x_b at approximately 4 diameters, and x_c at approximately 5 diameters. These longitudinal positions were then used as fixed positions for both nozzles regardless of changes in flap position or movement of the wing relative to the engine.

Tests were made with each nozzle configuration at two positions of the wing with respect to the engine (y-dimensions (fig. 5)). The conical nozzle was positioned as close to the wing as possible (y_d) at longitudinal position x_a. The daisy nozzle was positioned as close to the wing as possible (y_e) at longitudinal position x_a, but because of the larger diameter of the nozzle, the centerline was 0.102 meter (4 inches) farther away from the wing than the centerline of the conical nozzle. The second position of the

conical nozzle coincided with the closest position of the daisy nozzle, so that the centerlines of both nozzle configurations were at y_e. The second position of the daisy nozzle was the same increment of distance away (0.102 m (4 in.)) from the closest position as y_e was for the conical nozzle. No data were taken at the conical nozzle position closest to both the wing and the flap (x_a, y_d).

Measured thrust. – The thrust of the engine was measured, using the thrust table and its underground balance system, with each exhaust nozzle configuration installed. Measured engine thrust, F_m, is plotted against corrected fan rotor speed, $\frac{N_f}{\sqrt{\theta}}$, in figure 6. The resultant curve represents the thrust of both nozzle configurations for all the tests, which were conducted at an elevation of 701 meters (2300 feet).

Instrumentation

Static pressure ports were installed in the wing, vane, and flap, providing low response steady-state pressures in a grid as shown in figures 2(a) to 2(c). Each of these static pressure ports was connected to a 48-port rotating valve that could sense, on one pressure transducer, the differential between the sensed pressure and the ambient reference pressure every 2.5 seconds. Data from each of these pressure ports were coded for data reduction by a pulse code modulation (PCM) system.

At three static pressure port locations on the flap (p_u, p_v, and p_w) on or near the centerline of jet exhaust impingement, high response transducers were mounted so that their diaphragms were flush to the surface of the flap (fig. 2(a)). These transducers were capable of withstanding the high temperatures of the jet exhaust. The output from each of the transducers was recorded on individual analog FM magnetic tape tracks.

Temperature measurements were obtained at each static pressure port, as shown in the sketch in figure 2(a), by means of surface-mounted thermocouples. Data from each temperature thermocouple were coded for data reduction by a PCM system.

DATA REDUCTION AND ANALYSIS

The data reduction process consisted of formatting and digital processing by arranging the commutated PCM data into a compatible format. The digital processing included instrumentation calibration and tabular listout of all data in engineering units averaged over the period of the steady-state run conditions.

The high response pressure data were analyzed on a narrow band (8 Hz) spectrum analyzer and time-averaged on a high dynamic range digital averager. Power spectral density (PSD) information was obtained for each pressure trace during each data run over the frequency range of 5 hertz to 500 hertz, and results were printed out on an automatic plotter coupled to the spectrum analyzer.

ACCURACY

The approximate maximum errors in important measured and derived quantities were as follows:

Parameter	Maximum error
F_m	±222 N (±50 lbf)
p/p_o	±1 percent of value
T	±3° C (±5° F)
F_p	±5 percent of value

RESULTS AND DISCUSSION

Pressure and Temperature Profiles

Pressure and temperature data obtained during the ground tests of the externally blown flap system were plotted on scale drawings of the test wing at corresponding recording locations. Lines of equal pressure or temperature were then drawn between the plotted data points. A typical set of contour curves showing pressure and temperature profiles with the flap at the 60° position for both nozzle configurations is shown in figures 7(a) to 7(d). Temperature and pressure contour drawings of this type were made for each stabilized data run and were used to determine quantitatively the effects of exhaust impingement. The pressure contours were also integrated for each stabilized data run to determine the overall pressure load on the underside of the flap and vane. The wing surface pressure and temperature contours did not reveal any unusual or extreme values like those on the flaps and vanes. Consequently, no analysis was made of the wing surface.

The maximum pressures and temperatures recorded during each data run are plotted against corrected fan rotor speed, $\frac{N_f}{\sqrt{\theta}}$, for both nozzle configurations in figure 8. The maximum pressures recorded on the flap for the conical nozzle are higher over the range of $\frac{N_f}{\sqrt{\theta}}$ than the pressures recorded with the daisy nozzle (fig. 8(a)). This indicates a greater concentration or focusing of exhaust pressure with the conical nozzle configuration. This concentration is confirmed in figure 8(b), which shows that the maximum temperatures recorded on the flap are higher with the conical nozzle than with the daisy nozzle. The maximum temperature measured on the flaps occurred when the engine was closest to the wing and closest to the flap for both nozzle configurations. With an engine exhaust gas temperature of 315° C (600° F) at the exhaust exit, the maximum temperature recorded on the flap was 218° C (424° F) for the

conical nozzle and 180° C (356° F) for the daisy nozzle. It should be noted that these maximum temperatures occurred with no flow over the wing and flap; under actual flight conditions the temperatures would probably be lower.

Lower Surface Flap Loads

The load experienced by the lower surface of the flap as a result of engine exhaust impingement was determined by integrating the static pressure contour data for each steady-state data run at flap positions of 35° and 60°. With the flaps retracted, the load on the flaps was essentially zero.

Effect of flap position.—A plot of lower surface flap loads, F_p, against flap position is shown in figures 9(a) and 9(b) for a corrected fan rotor speed of approximately 7300 rpm at three longitudinal engine locations relative to the flap (x_a, x_b, and x_c) and at three engine positions relatively close to the wing (y_d, y_e, and y_f). For the conical nozzle configuration, the F_p at all the wing/engine relationships is within a spread of 445 newtons (100 pounds force) at the 35° flap position and within 667 newtons (150 pounds force) at the 60° flap position. For the daisy nozzle configuration, F_p is within 445 newtons (100 pounds force) at the 35° flap position and within 1001 newtons (225 pounds force) at the 60° flap position. Even though the values of F_p at the 35° and 60° flap positions varied somewhat with the different nozzle configurations, figure 9 shows that for both configurations the loads on the undersurface of the flap at the 60° flap position are approximately three times as great as those at the 35° flap position.

Effect of engine/wing position.—The effect of longitudinal engine position (x_a, x_b, or x_c) on F_p at several fan rotor speeds with the engine at three positions relatively close to the wing (y_d, y_e, and y_f) is shown in figure 10. For the daisy nozzle configuration, F_p generally increases as the engine is moved from longitudinal engine position x_c to x_b (closer to the flap). When the engine is moved to x_a, F_p continues to increase, except at two power settings where there is a slight decrease; however, F_p at the x_a position is greater than F_p at the x_c position for all the test conditions. For the conical nozzle configuration at the 60° flap position, moving the nozzle closer to the flap (from x_c to x_a) causes a general increase in F_p except at the maximum engine rotor speed.

Positioning the engine closer to the wing did not always cause an increase in F_p. In figure 10, as the daisy nozzle moves from x_c to x_a, the triangles are generally above the squares, indicating that F_p increases as the engine moves farther from the wing and, in general, decreases as the engine moves closer to the wing.

Effect of engine thrust.—Although F_p can be correlated generally with fan rotor

speed, it is desirable to determine the values of thrust generated by the engine (fig. 6) and to correlate these values with the actual pressure loads measured on the undersurface of the flaps as a result of the impingement of the engine exhaust gas. Figures 11(a) to 11(c) show the F_p measured on the flap and vane for both nozzle configurations and at all engine/wing positions for the 60° and the 35° flap positions. The curves show that as the measured engine thrust, F_m, increases, F_p for the flap and vane also increases. Figure 11(a) also shows a reduction in the rate of increase of $F_{p,\,flap}$ with increasing thrust above a thrust level of 12,233 newtons (2750 pounds force) with the conical nozzle for all but the x_c, y_e position. For the daisy nozzle (fig. 11(b)), the only conditions that provide such a reduction are the combinations x_c, y_e and x_b, y_f.

The F_p per unit of measured thrust is plotted for all the test conditions for the daisy nozzle configuration in figure 12(a) and for the conical nozzle configuration in figure 12(b). These figures show that F_p was a fairly constant percentage of the measured thrust. For the test conditions with the 60° flap position, the maximum F_p transmitted to the flap was about 55 percent of the measured thrust for both nozzle configurations and was more than 40 percent of the measured thrust over the entire thrust range.

Spanwise distribution. – The spanwise flap F_p was determined by dividing the flap into 10 segments of equal length and integrating the faired pressures in each segment. This was done for several nozzle positions with the flaps positioned at 60° for both nozzle configurations. The load on each 10-percent segment of the span was calculated as a percentage of the total load for each configuration. The percentage distribution of F_p over the span of the flap for three engine/wing positions is shown in figures 13(a) and 13(b). The conical nozzle tended to concentrate most of the pressure load on one 10-percent segment of the flap, but the daisy nozzle spread the pressure load more evenly over more than one segment. For the conical nozzle configuration, a maximum F_p of 37 percent was concentrated on the 10-percent segment of the flap near the engine exhaust centerline. The F_p produced by the daisy nozzle configuration was concentrated on two adjacent 10-percent flap segments straddling the engine centerline and was approximately 30 percent on each segment. For either nozzle configuration, more than 90 percent of the F_p on the flap was within ±20 percent of the flap span centered around the exhaust centerline.

Dynamic Pressure Measurements

Power spectral density traces obtained for the high response pressures on the flap surface were analyzed over the frequency range from 5 hertz to 500 hertz for many of the steady-state data runs. Attempts were made to correlate the power spikes in the PSD curves from each data run with the fan or core rotor speeds and the blade passage frequencies. Figures 14(a) and 14(b) show PSD traces obtained from two transducers on the surface of the flaps which were deflected 35°. The data were obtained with the

daisy nozzle at engine/wing positions of x_c, y_e and x_c, y_f and for a range of rotor speeds from approximately 76 to 122 rps for the fan rotor and approximately 200 to 250 rps for the core rotor. The frequencies of the peak PSD values do not vary as much as the change in rotor speed of 50 cps, thus the peak frequencies in the PSD traces are not related to the fan or core rotor speeds or to blade passage frequencies.

The PSD curves of figures 14(a) and 14(b) show the difference in frequency values at the peak PSD value recorded by the two transducers for the same data runs. These transducers were only 0.305 meter (12 inches) apart on the flap and were both in the engine exhaust impingement area, yet they recorded peak frequencies which differed by about 50 cps. Differences in panel stiffness or proximity to major flap structure could account for the disparity in peak frequencies, which would indicate that the transducers were sensitive to flap accelerations or vibrations.

SUMMARY OF RESULTS

Pressure and temperature data were measured on the undersurface of an F-111B wing, vane, and flap which were used in conjunction with a CF700 engine to simulate an externally blown flap system. The angle of incidence between the engine and the wing was fixed at 3° during the tests, and there was no airflow over the wing. Two engine exhaust nozzles (conical and daisy) and several wing/engine positions, engine thrust levels, and flap positions were used.

The pressure load obtained by integrating the local pressures on the undersurface of the flap, F_p, produced loads that were approximately three times greater at the 60° flap position than at the 35° flap position for equivalent thrust settings.

The value of F_p generally increased as the engine was moved closer to the flap and as corrected fan rotor speed was increased, but not as the engine was moved closer to the wing.

At the specified test conditions and for a 60° flap position, the maximum F_p transmitted to the flap was 55 percent of the engine thrust and more than 40 percent of the engine thrust over the test thrust range.

With an exhaust gas exit temperature of 315° C (600° F), the maximum temperatures recorded on the flaps were 180° C (356° F) for the daisy nozzle and 218° C (424° F) for the conical nozzle.

With the flaps in the 60° position, the maximum F_p measured on one 10-percent segment of flap span was 37 percent with the conical nozzle and approximately 30 percent on each of two adjacent segments with the daisy nozzle. More than 90 percent of the spanwise F_p on the flap was contained within ±20 percent of the flap span centered around the engine exhaust with both nozzle configurations.

The frequencies of the peak power spectral density values were not related to the fan or core rotor speeds or to blade passage frequencies for either nozzle configuration.

Flight Research Center,
National Aeronautics and Space Administration,
Edwards, Calif., July 7, 1972.

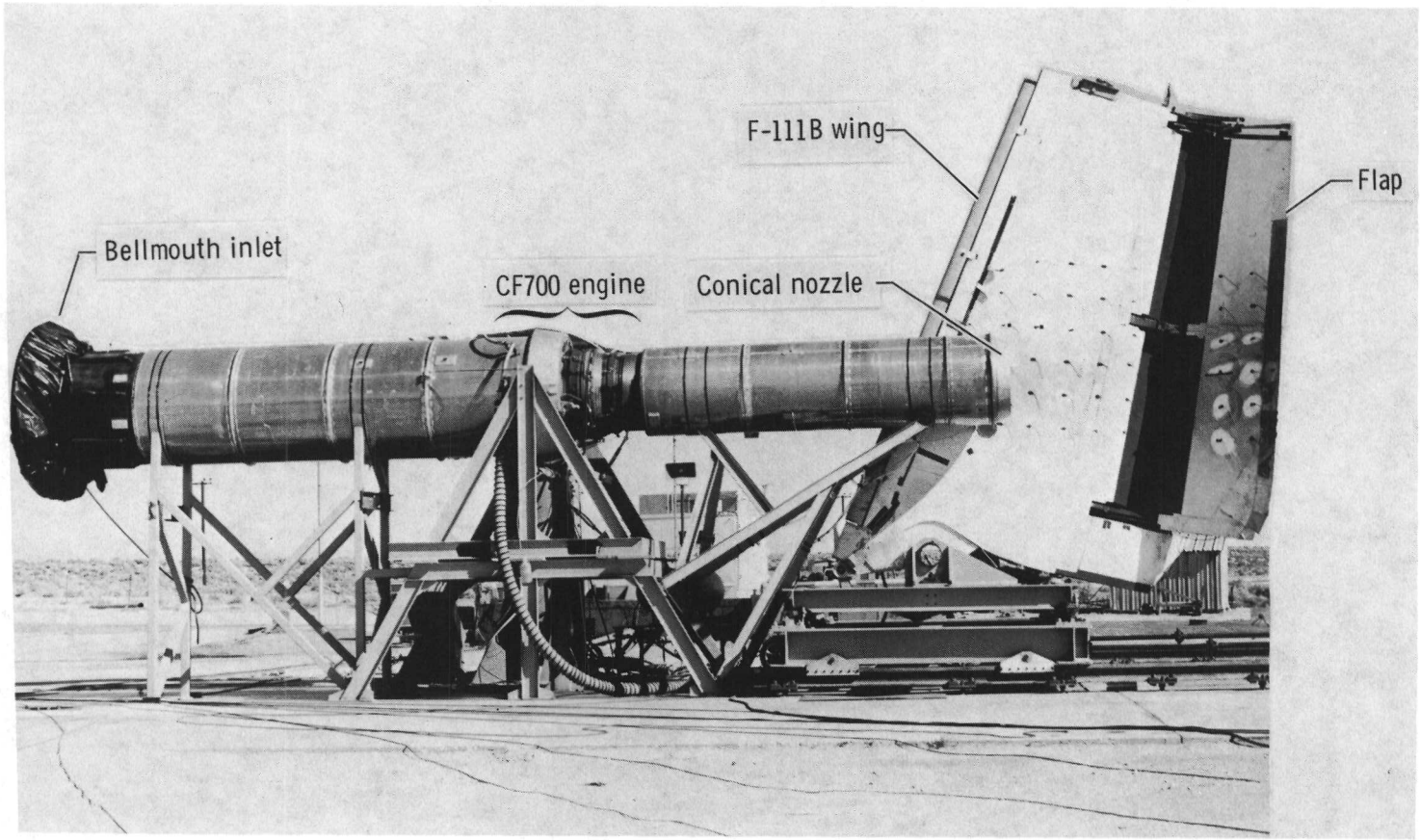

E-23296

Figure 1. F-111B wing and CF700 engine installed on the thrust stand with flaps deflected 60°, leading edge of wing swept 26°, and conical nozzle positioned at x_a, y_e.

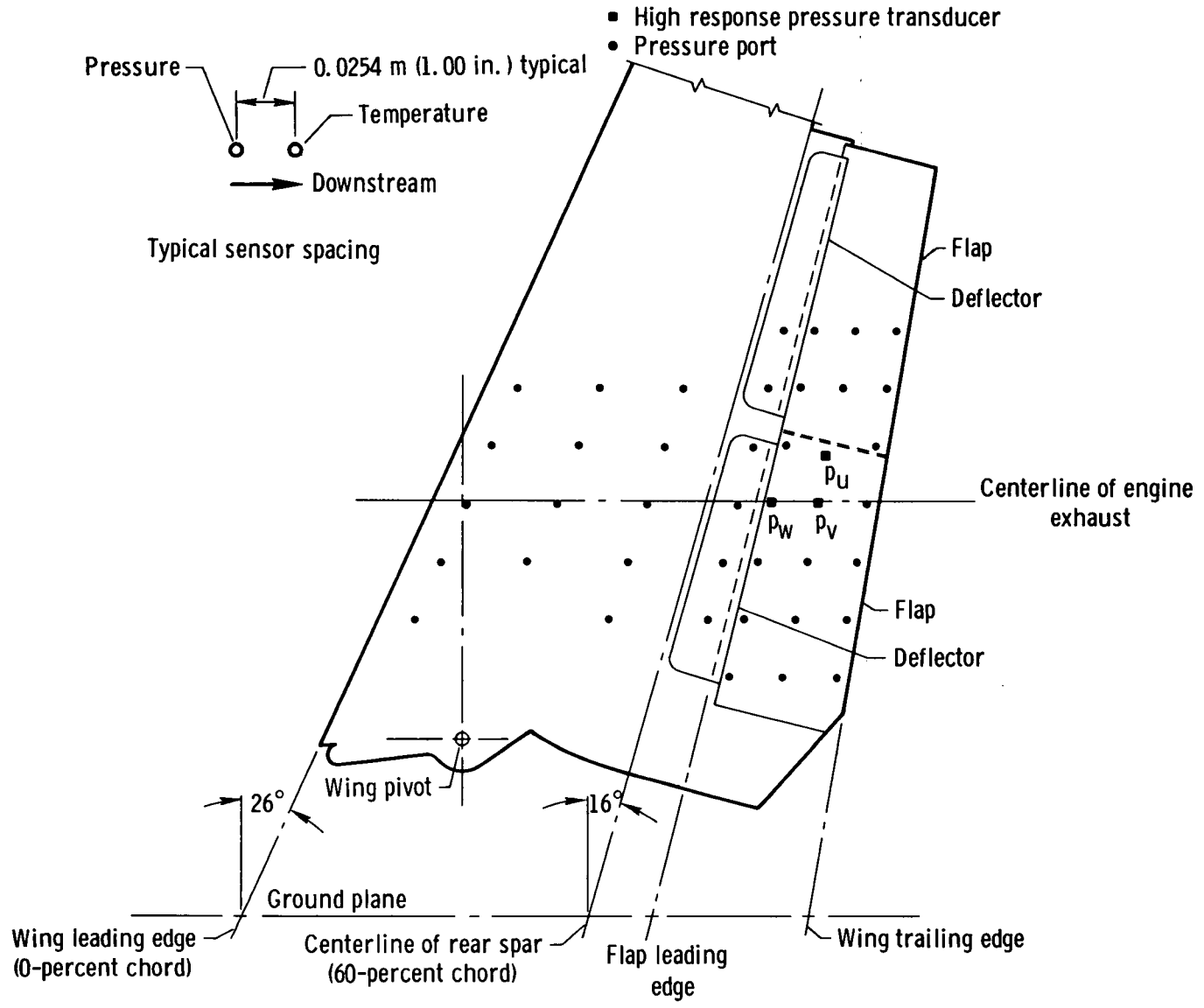

(a) Retracted flap.

Figure 2. F-111B wing undersurface showing pressure and temperature measurement locations with the flaps in the retracted, 35°, and 60° positions.

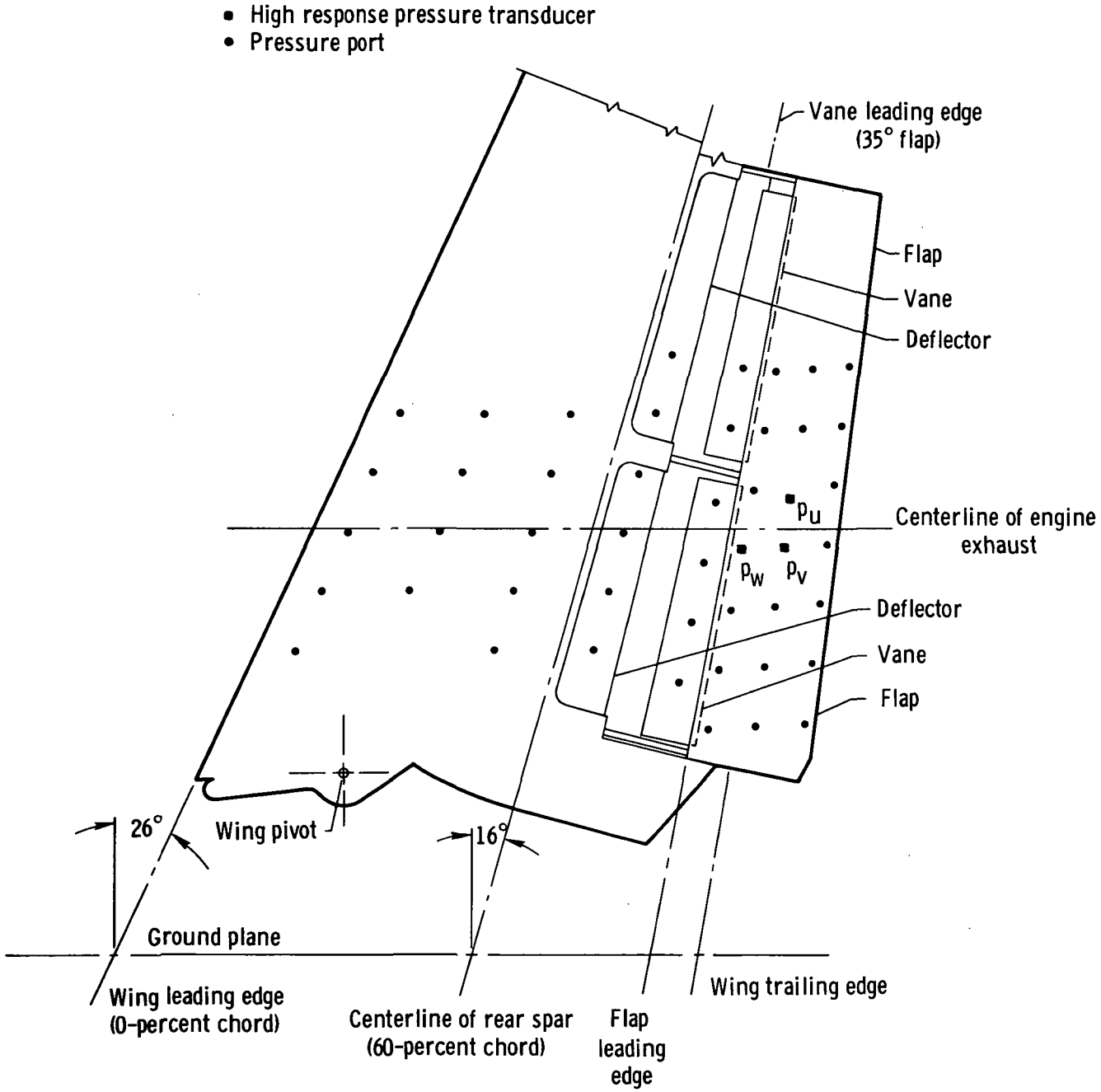

(b) 35° flap.

Figure 2. Continued.

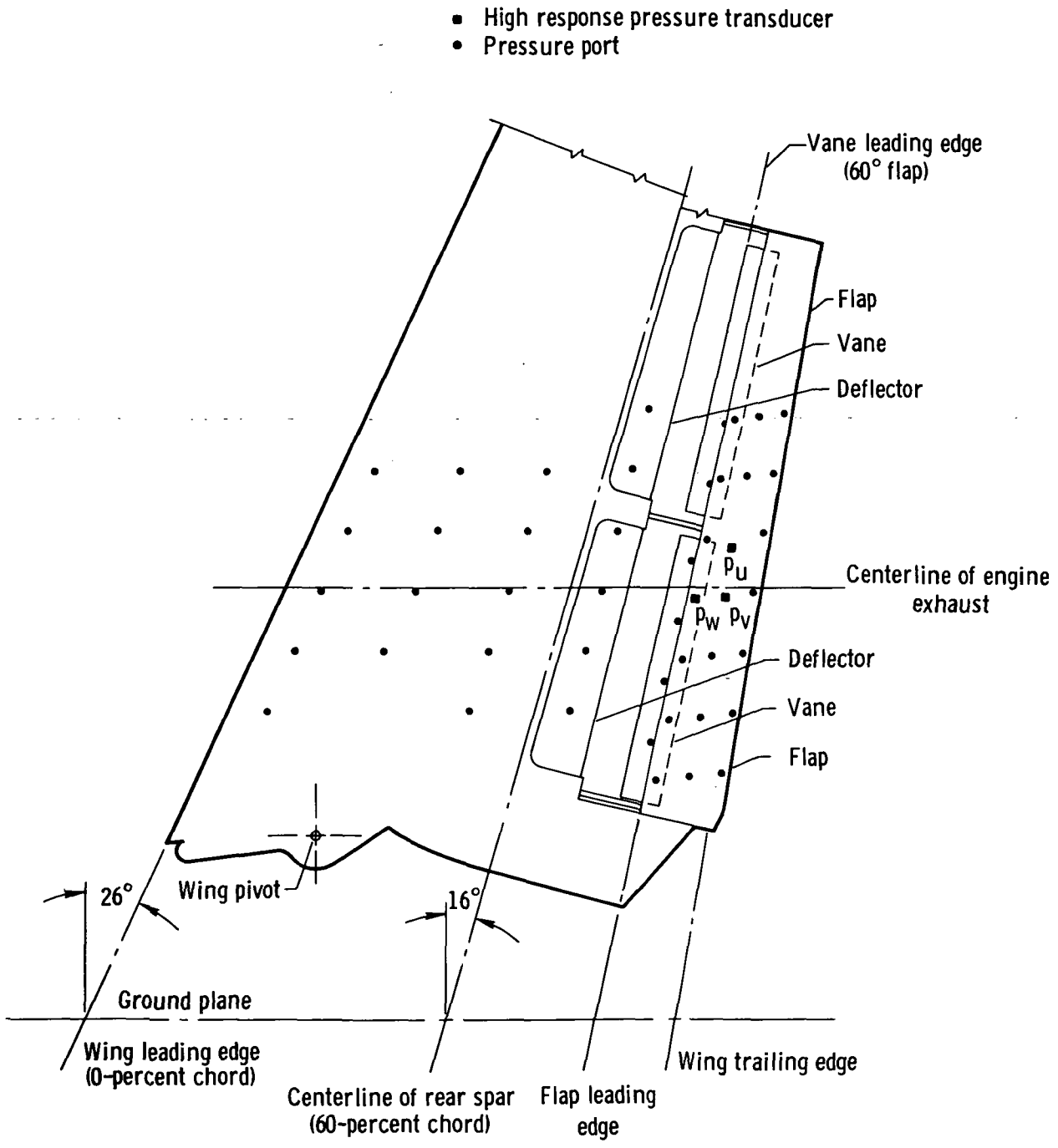

(c) 60° flap.

Figure 2. Concluded.

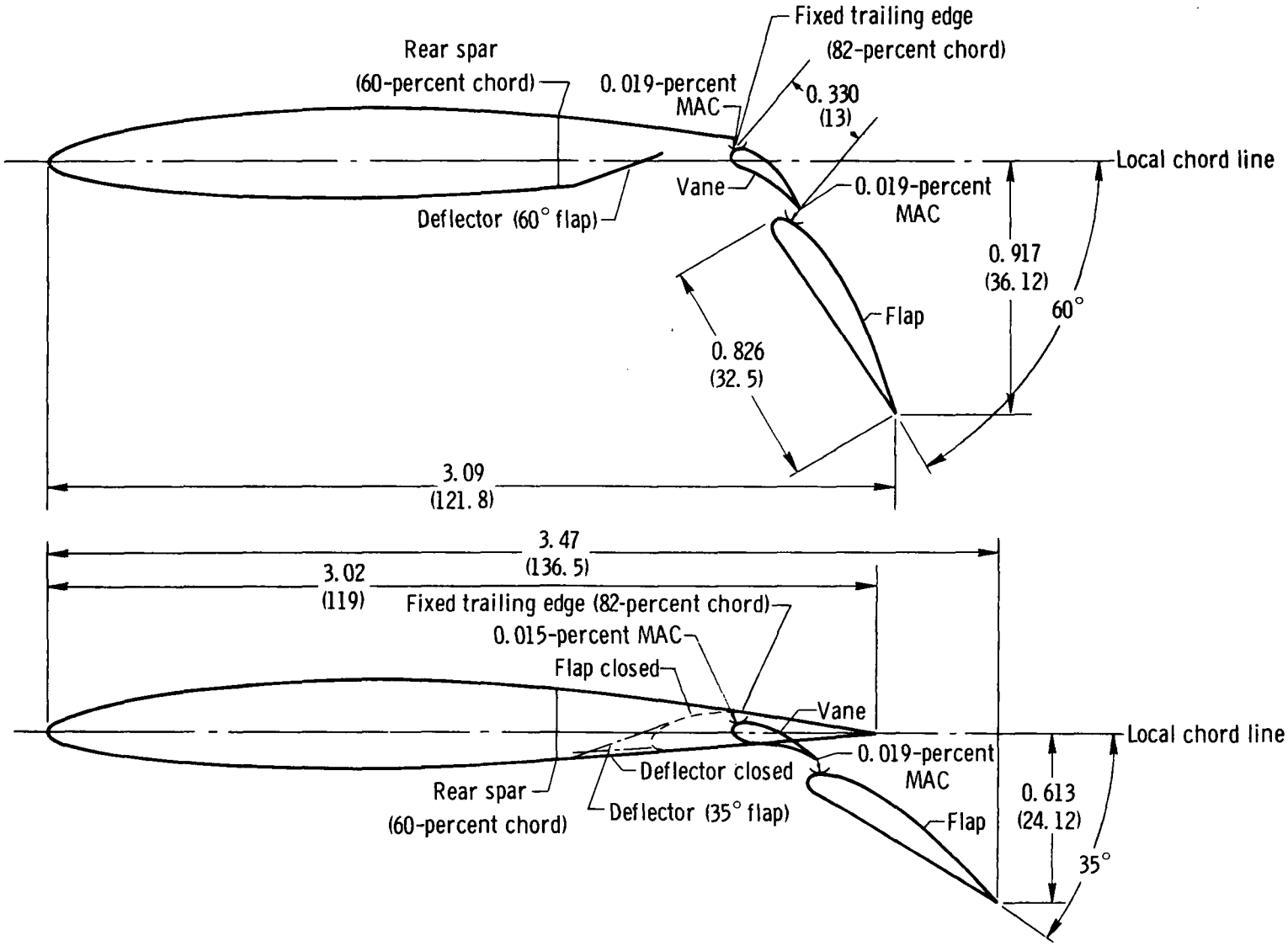

Figure 3. Sections through the F-111B wing and flap at exhaust centerline with the flaps in the retracted, 35°, and 60° positions. Dimensions in meters (inches); trailing edge flap chord, 25.8-percent wing chord; mean aerodynamic chord (MAC), 2.67 m (108.5 in.).

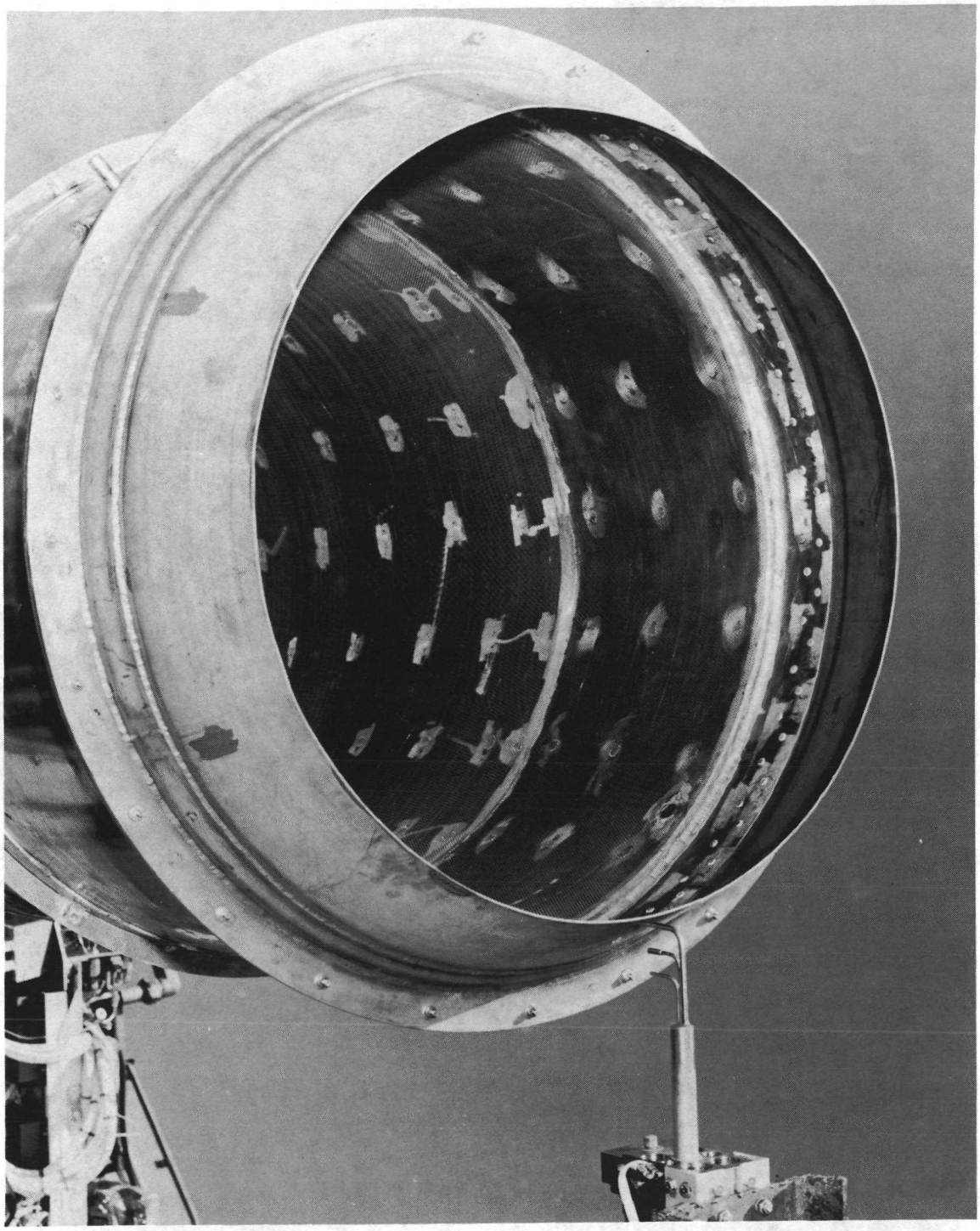

(a) Conical nozzle.

E-23308

Figure 4. Engine exhaust nozzle configurations used during ground tests of the externally blown flap system.

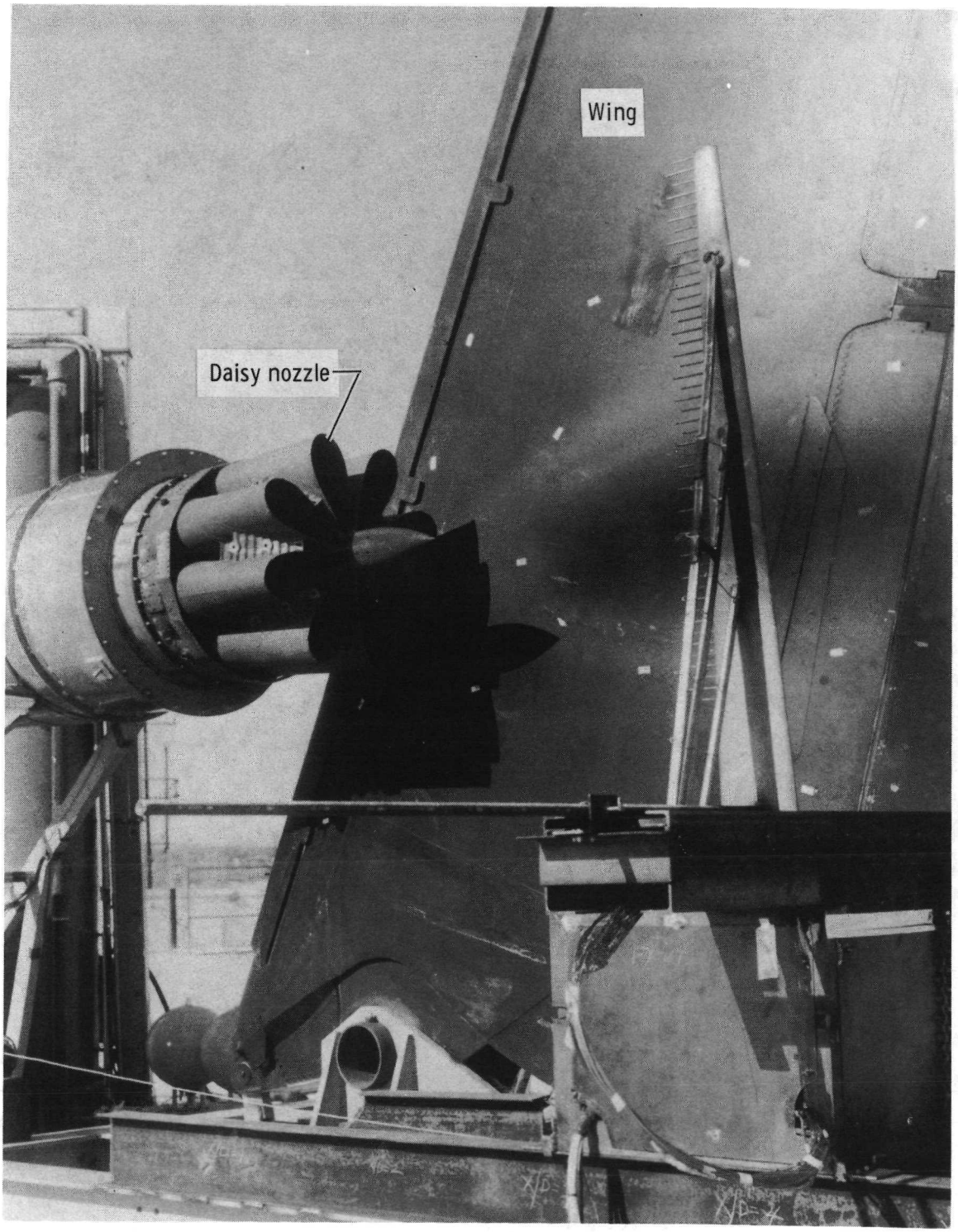

(b) Daisy nozzle.

Figure 4. Concluded.

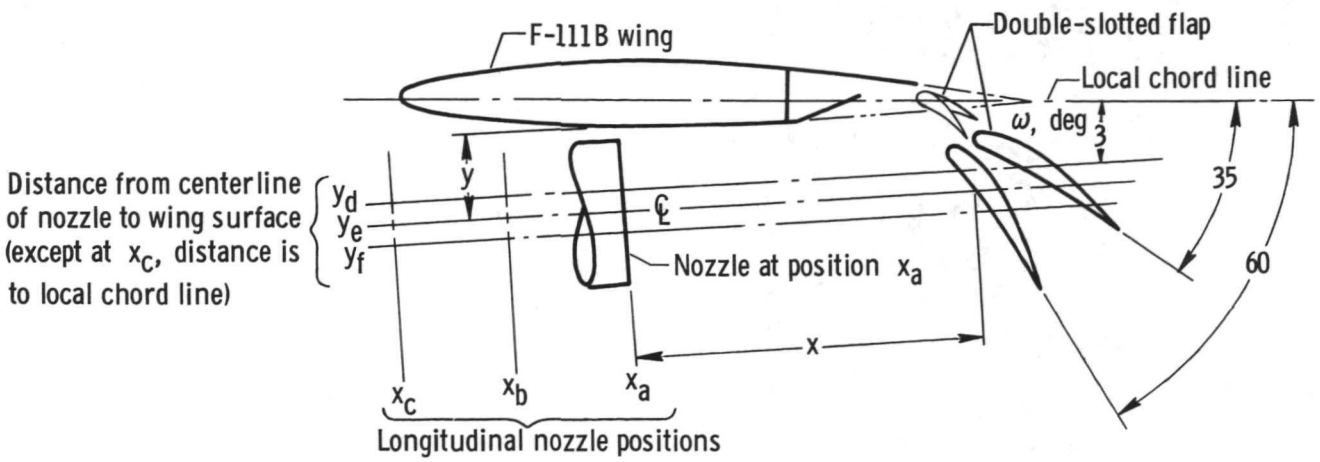

Nozzle		Nozzle position coordinates		35° and 60° flaps	60° flap	35° flap
				y, m (in.)	x, m (in.)	x, m (in.)
Conical	- - - -	y_d	x_b	0.356 (14)	2.184 (86)	2.464 (97)
	- - - -		x_c	.498 (19.6)	2.743 (108)	3.023 (119)
	Daisy	y_e	x_a	0.396 (15.6)	1.676 (66)	2.057 (81)
			x_b	.457 (18)	2.235 (88)	2.616 (103)
			x_c	.599 (23.6)	2.794 (110)	3.175 (125)
- - - - -		y_f	x_a	0.498 (19.6)	1.727 (68)	2.210 (87)
- - - - -			x_b	.559 (22)	2.286 (90)	2.769 (109)
- - - - -			x_c	.701 (27.6)	2.845 (112)	3.327 (131)

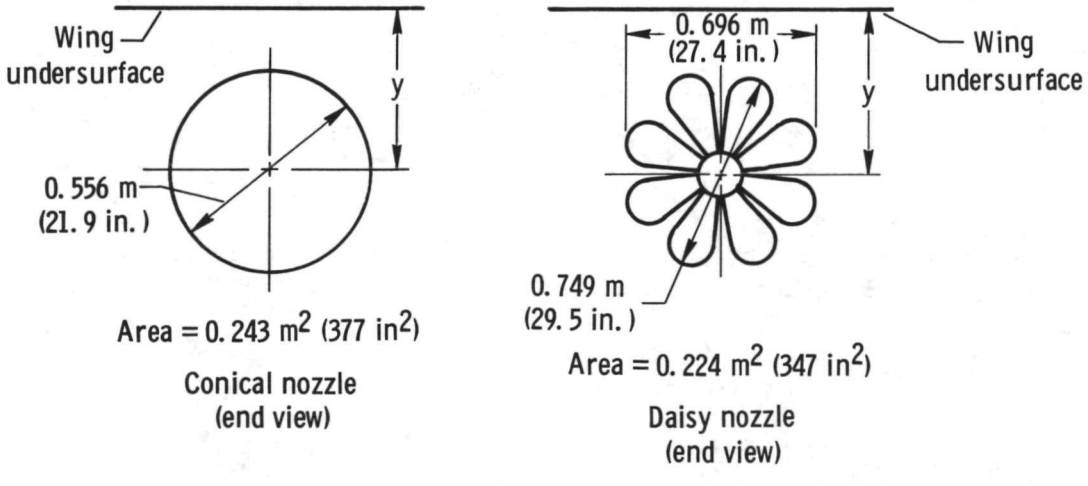

Figure 5. Wing, flap, and nozzle positions used in ground tests of the externally blown flap system.

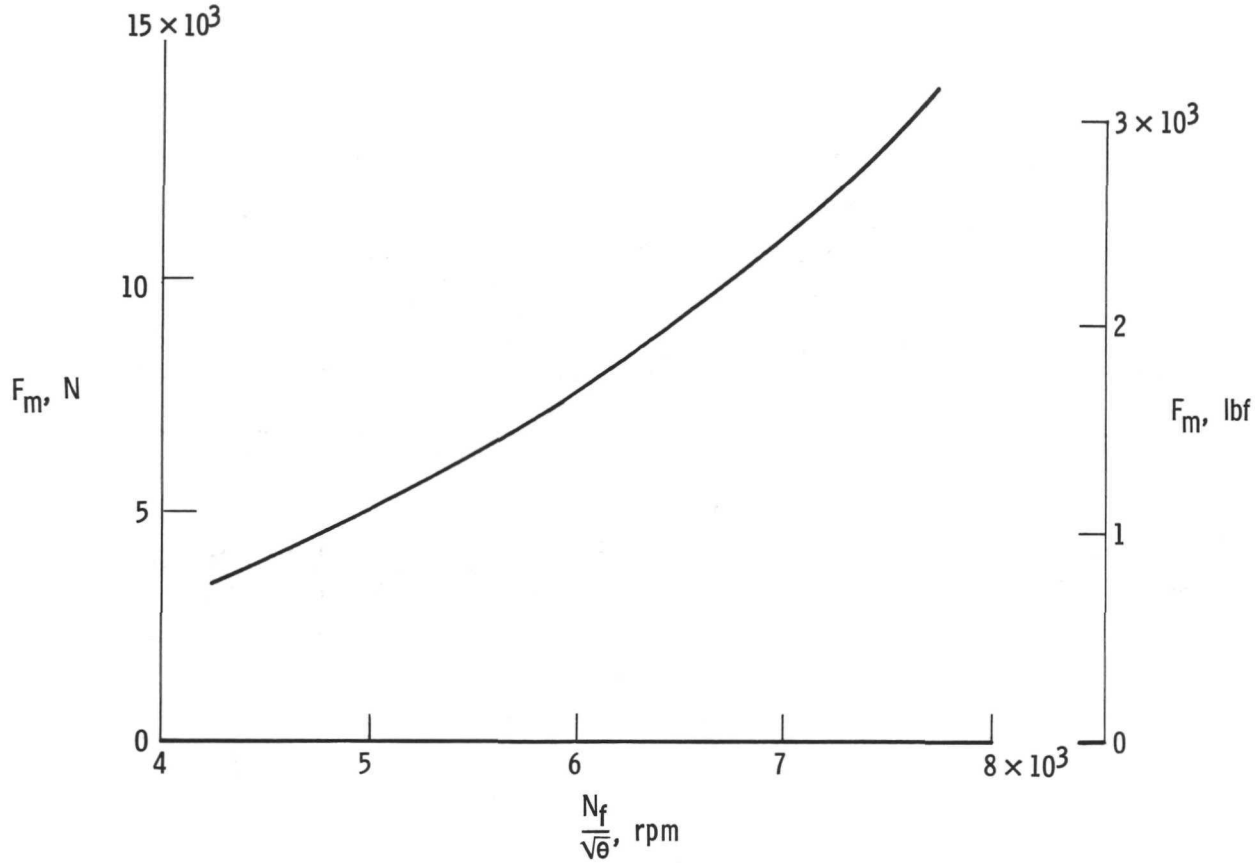

Figure 6. Measured engine thrust as a function of corrected fan rotor speed for the CF700 engine for both exhaust nozzle configurations at a test elevation of 701 meters (2300 feet).

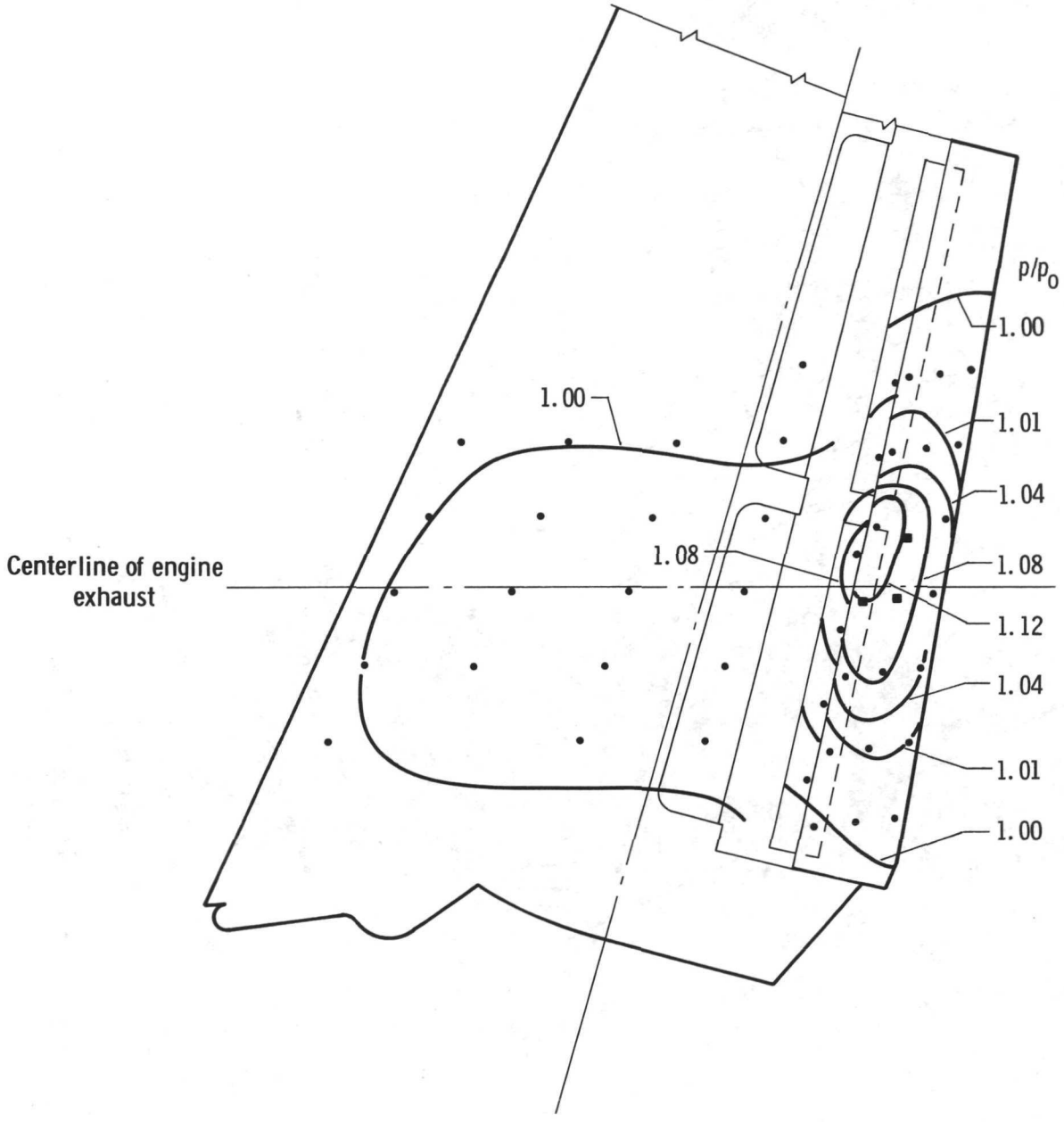

(a) Pressure profiles obtained with daisy nozzle at x_a, y_f. $\frac{N_f}{\sqrt{\theta}}$ = 8071 rpm;

p_o = 94122.4 N/m^2 (13.65 lbf/in^2); $F_{p,\,flap}$ = 8154 N (1833 lbf); $F_{p,\,vane}$ = 1877 N (422 lbf).

Figure 7. Plan views of wing undersurface showing typical pressure and temperature profiles with the flap deflected 60°.

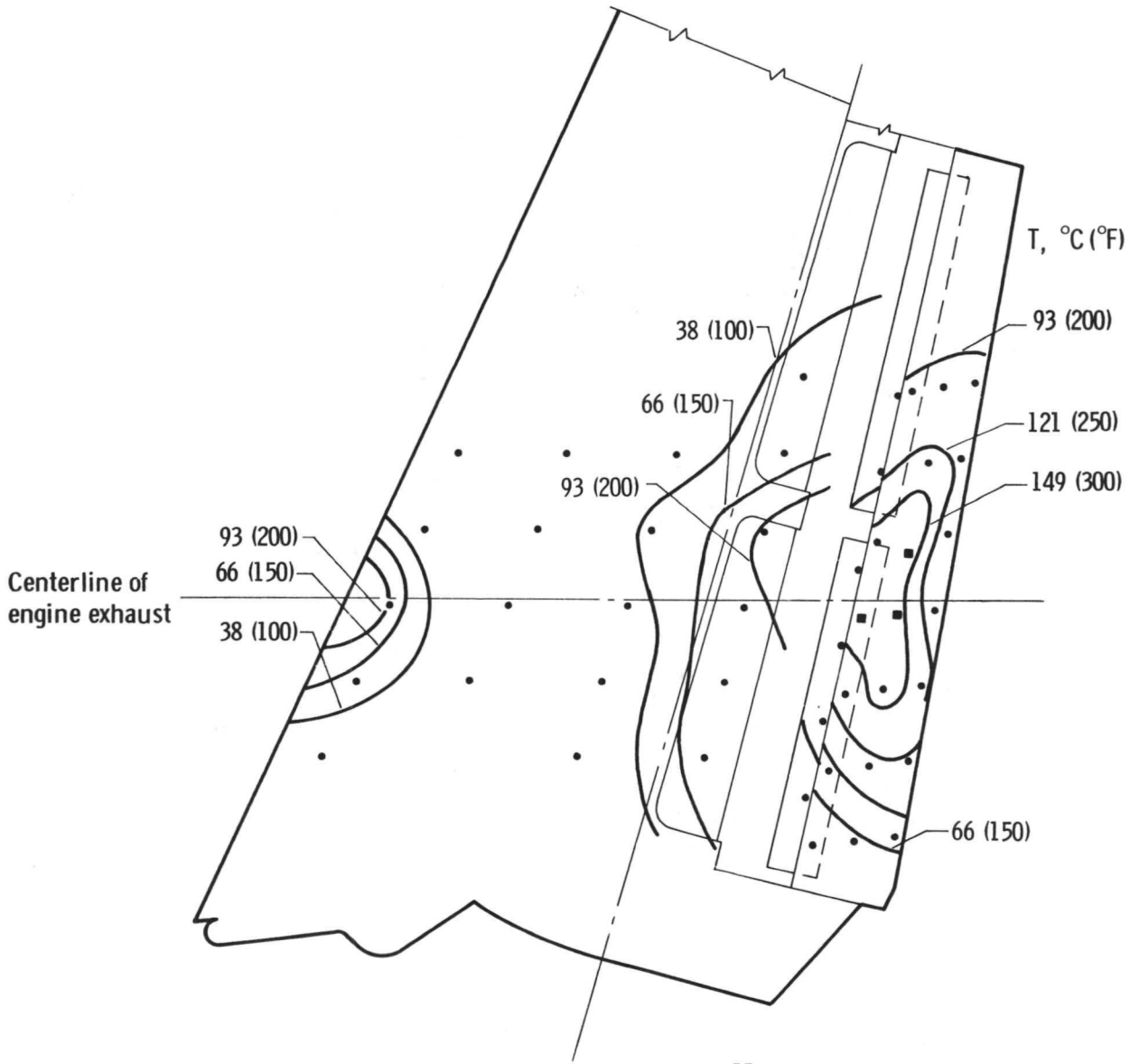

(b) Temperature profiles obtained with daisy nozzle at x_a, y_f. $\frac{N_f}{\sqrt{\theta}}$ = 8071 rpm; T_o = 1.94° C (35.5° F).

Figure 7. Continued.

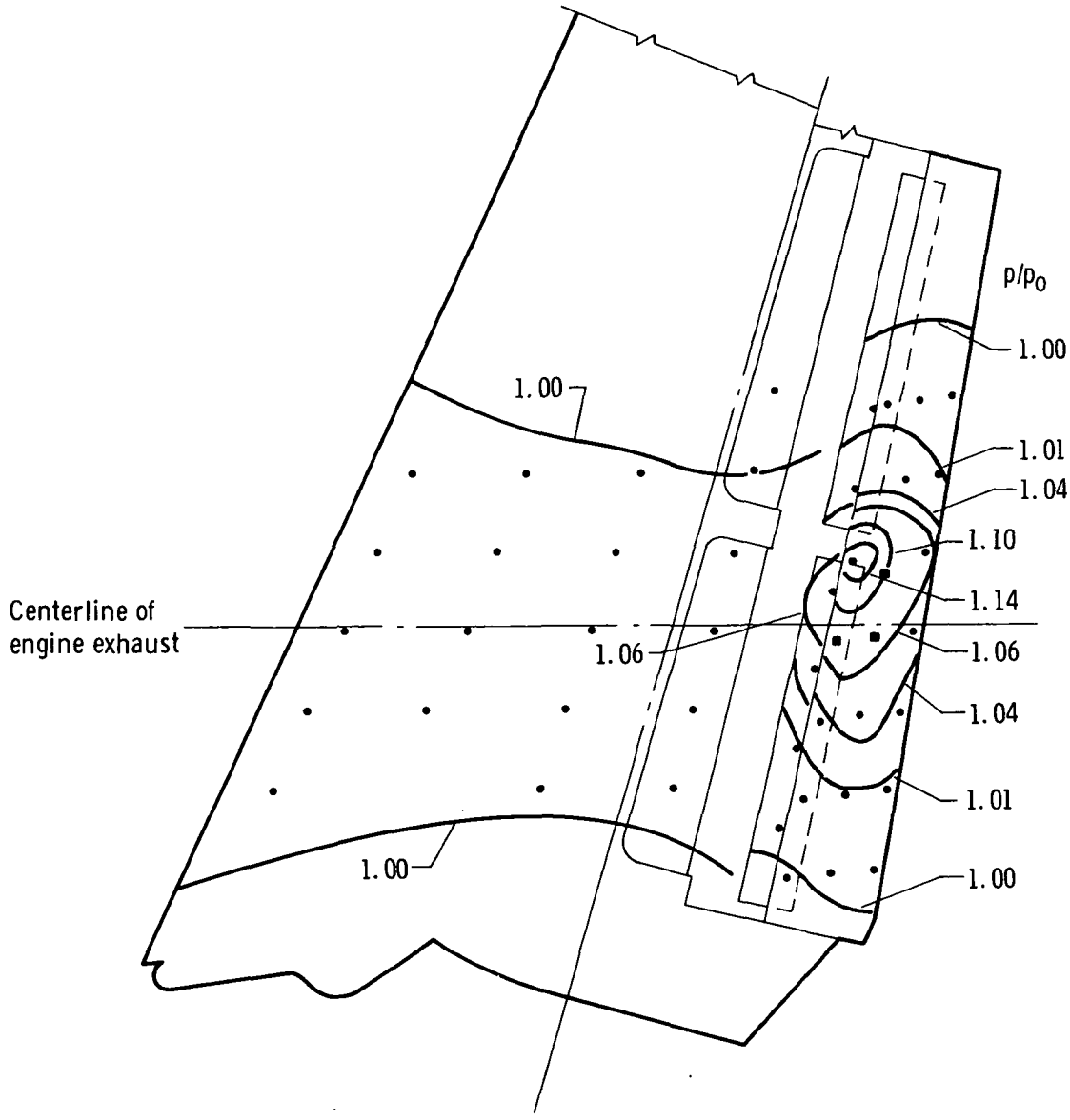

(c) Pressure profiles obtained with conical nozzle at x_a, y_e. $\frac{N_f}{\sqrt{\theta}}$ = 8078 rpm; p_o = 94122 N/m^2 (13.65 lbf/in^2); $F_{p,\,flap}$ = 7451 N (1675 lbf); $F_{p,\,vane}$ = 1463 N (329 lbf).

Figure 7. Continued.

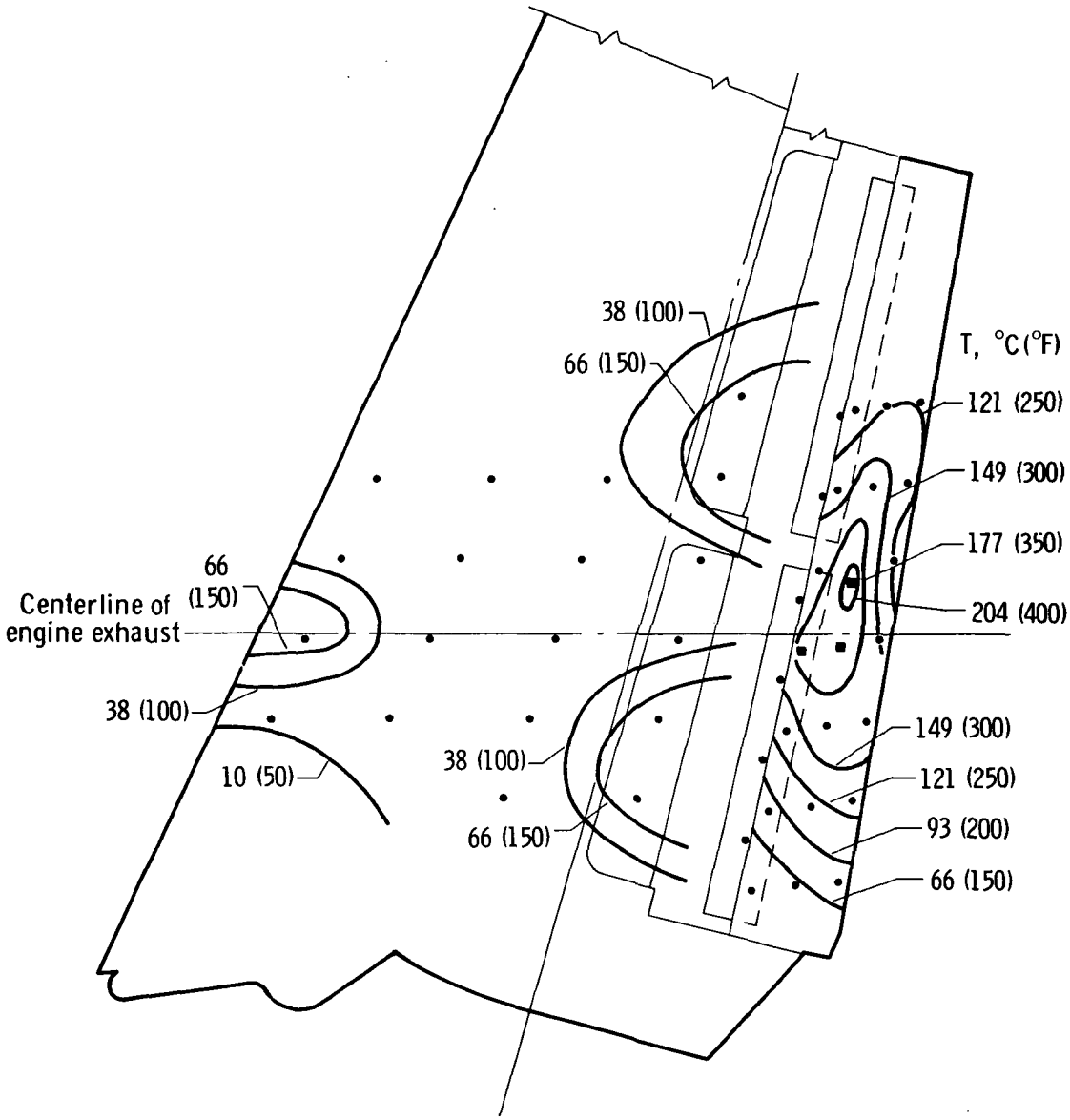

(d) Temperature profiles obtained with conical nozzle at x_a, y_e. $\frac{N_f}{\sqrt{\theta}}$ = 8078 rpm; T_o = -0.44° C (31.2° F).

Figure 7. Concluded.

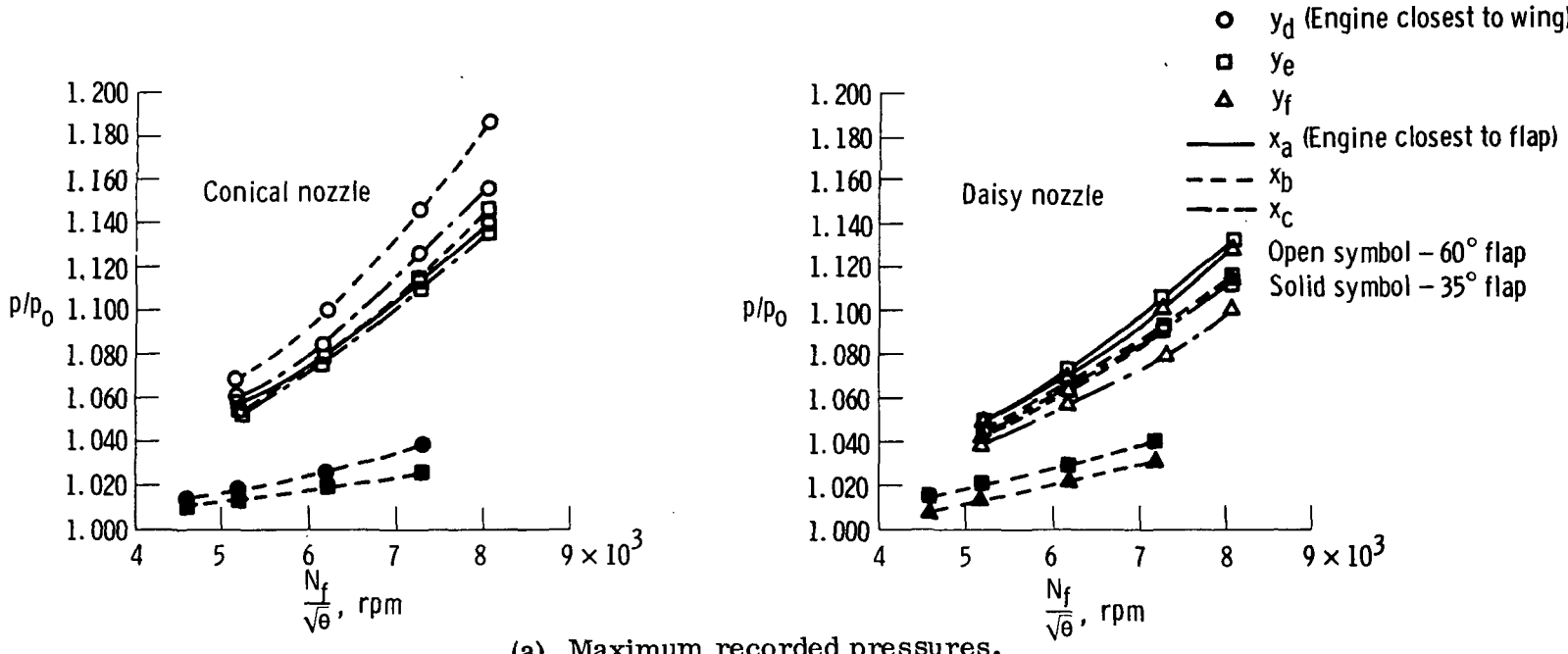

(a) Maximum recorded pressures.

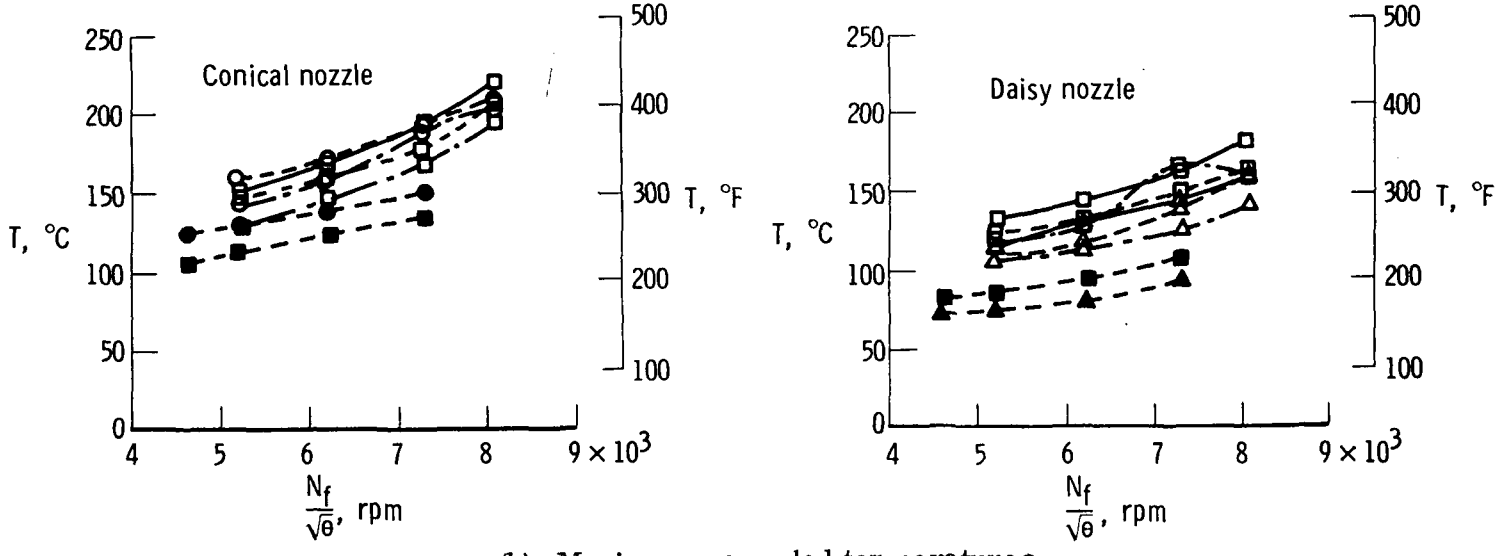

(b) Maximum recorded temperatures.

Figure 8. Effect of increasing corrected fan rotor speed on the maximum recorded pressures and temperatures on the flap for both nozzle configurations.

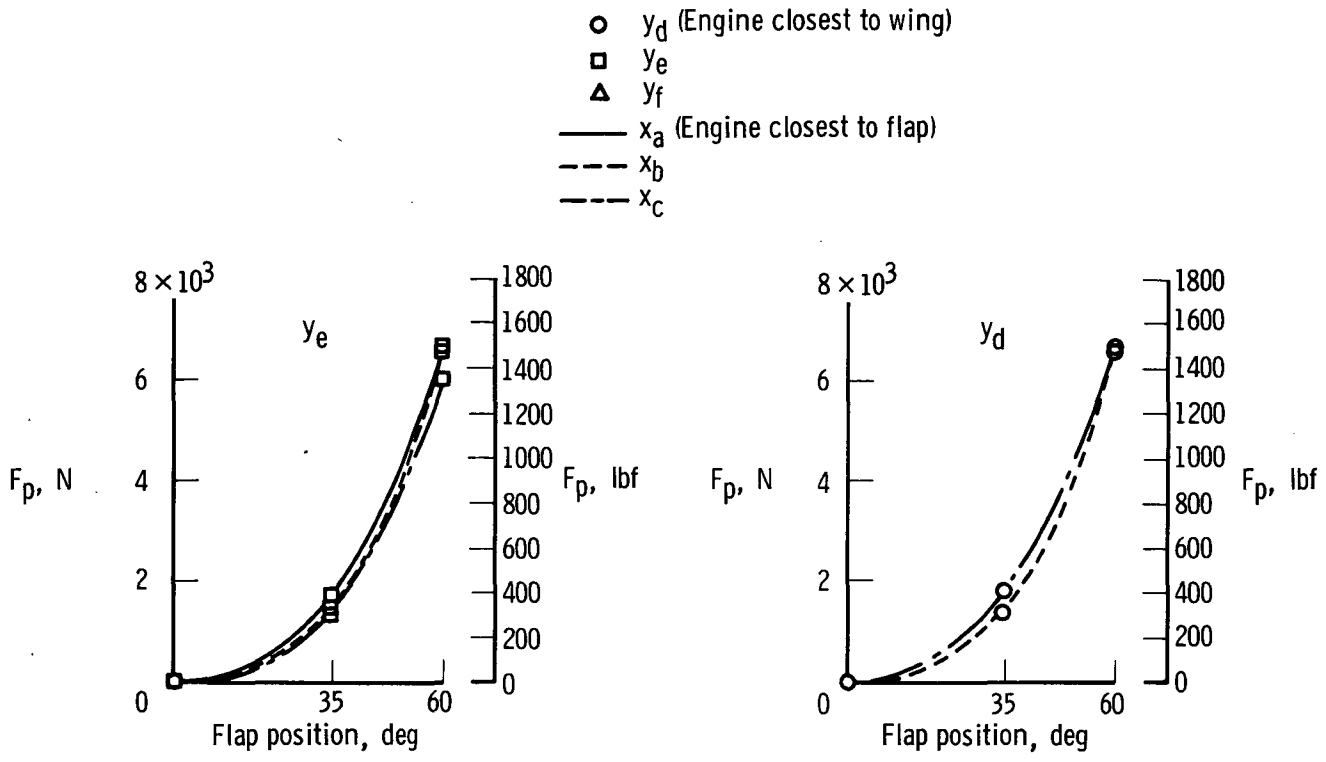

(a) Conical nozzle.

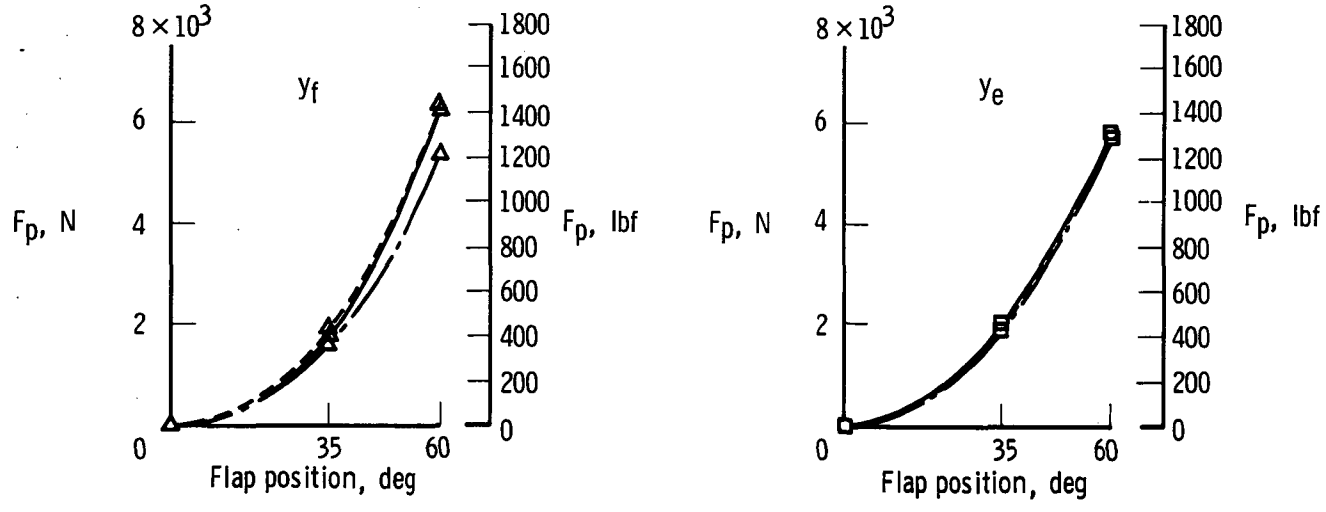

(b) Daisy nozzle.

Figure 9. Effect of flap position on F_p for both nozzle configurations at a corrected fan rotor speed of approximately 7300 rpm.

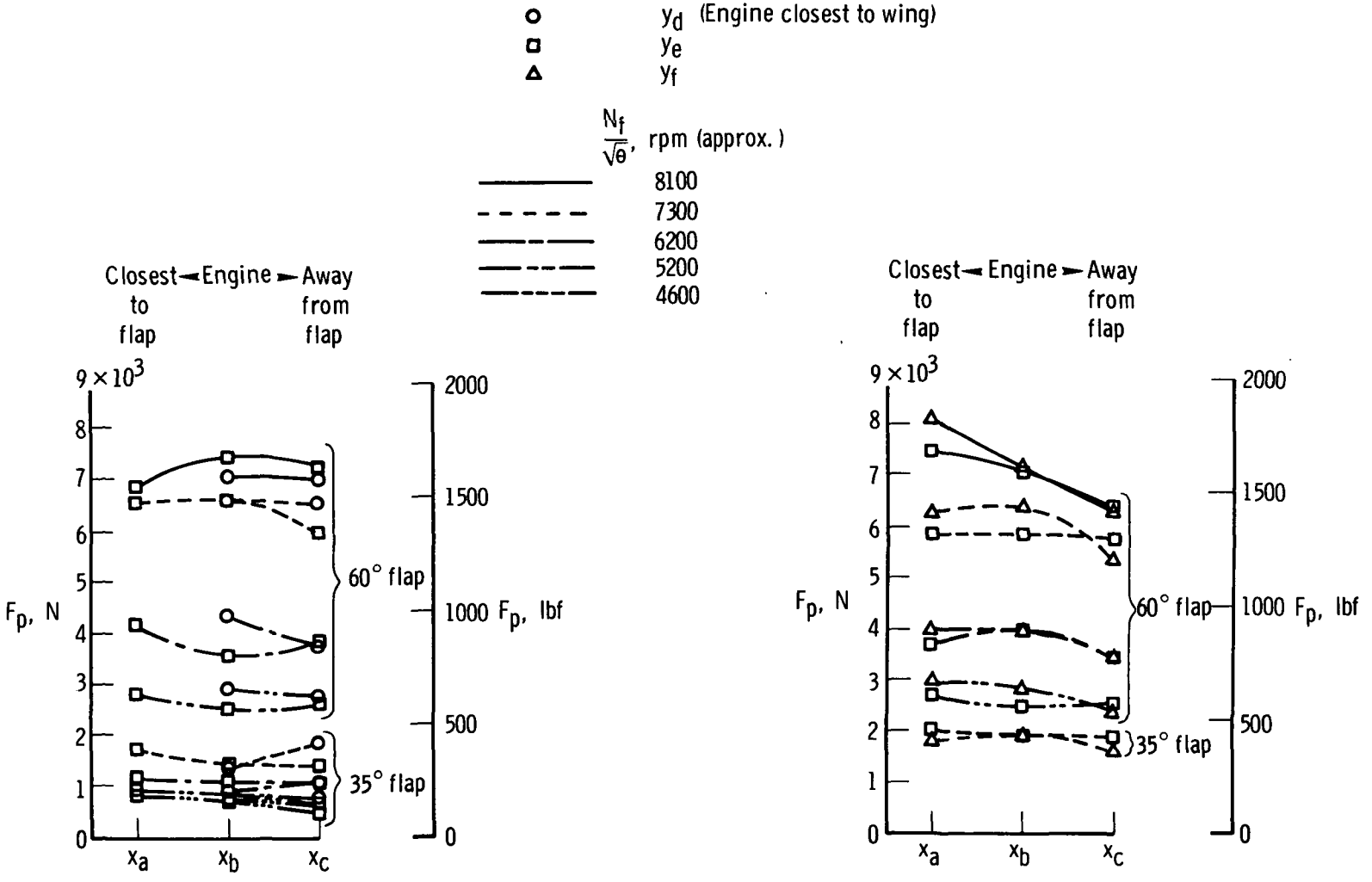

(a) Conical nozzle locations.

(b) Daisy nozzle locations.

Figure 10. Effect of engine exhaust nozzle location relative to wing and flap on F_p for a range of corrected fan rotor speeds.

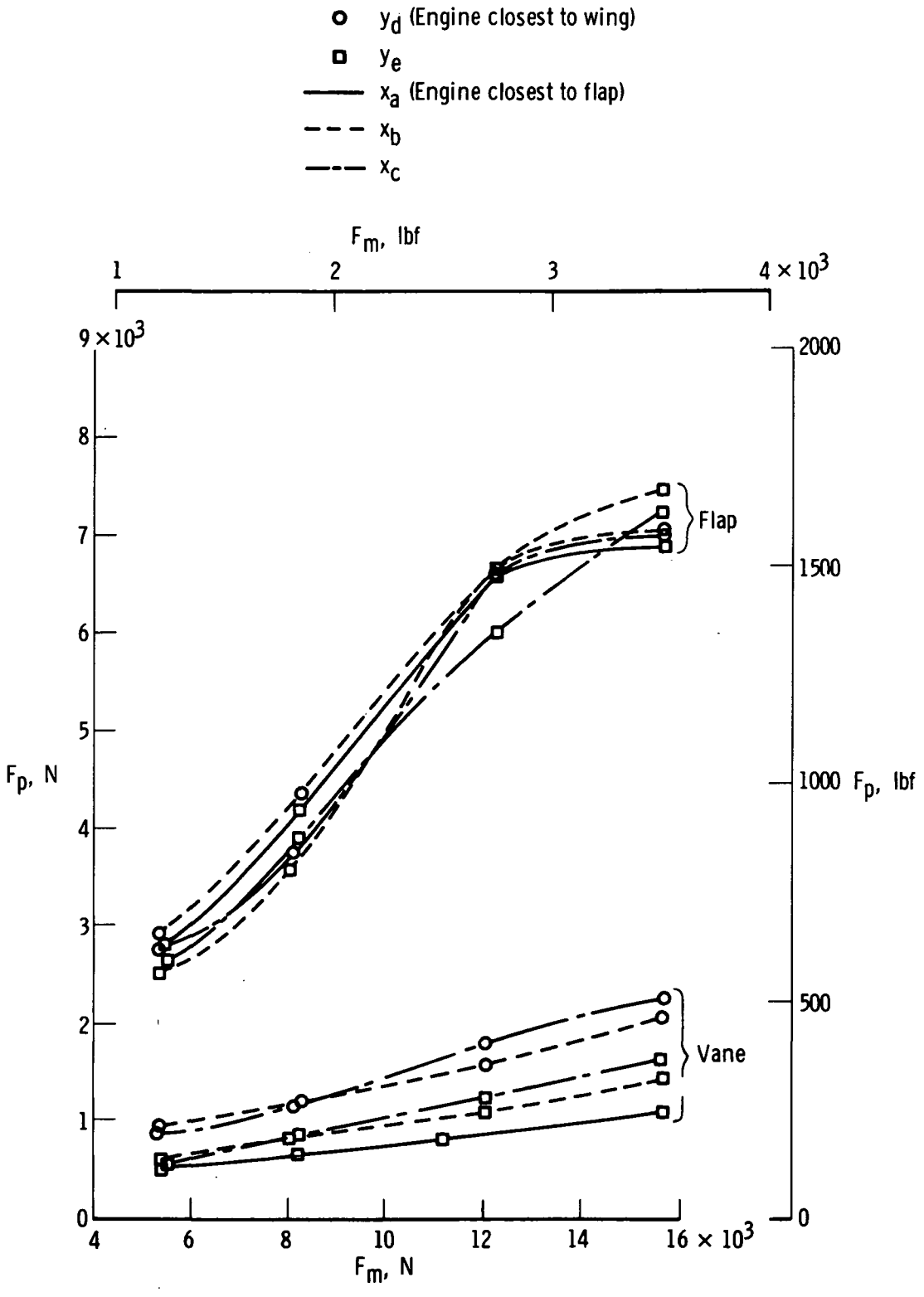

(a) Conical nozzle, flaps deflected 60°.

Figure 11. Effect of measured engine thrust on flap and vane loads for several engine exhaust nozzle locations.

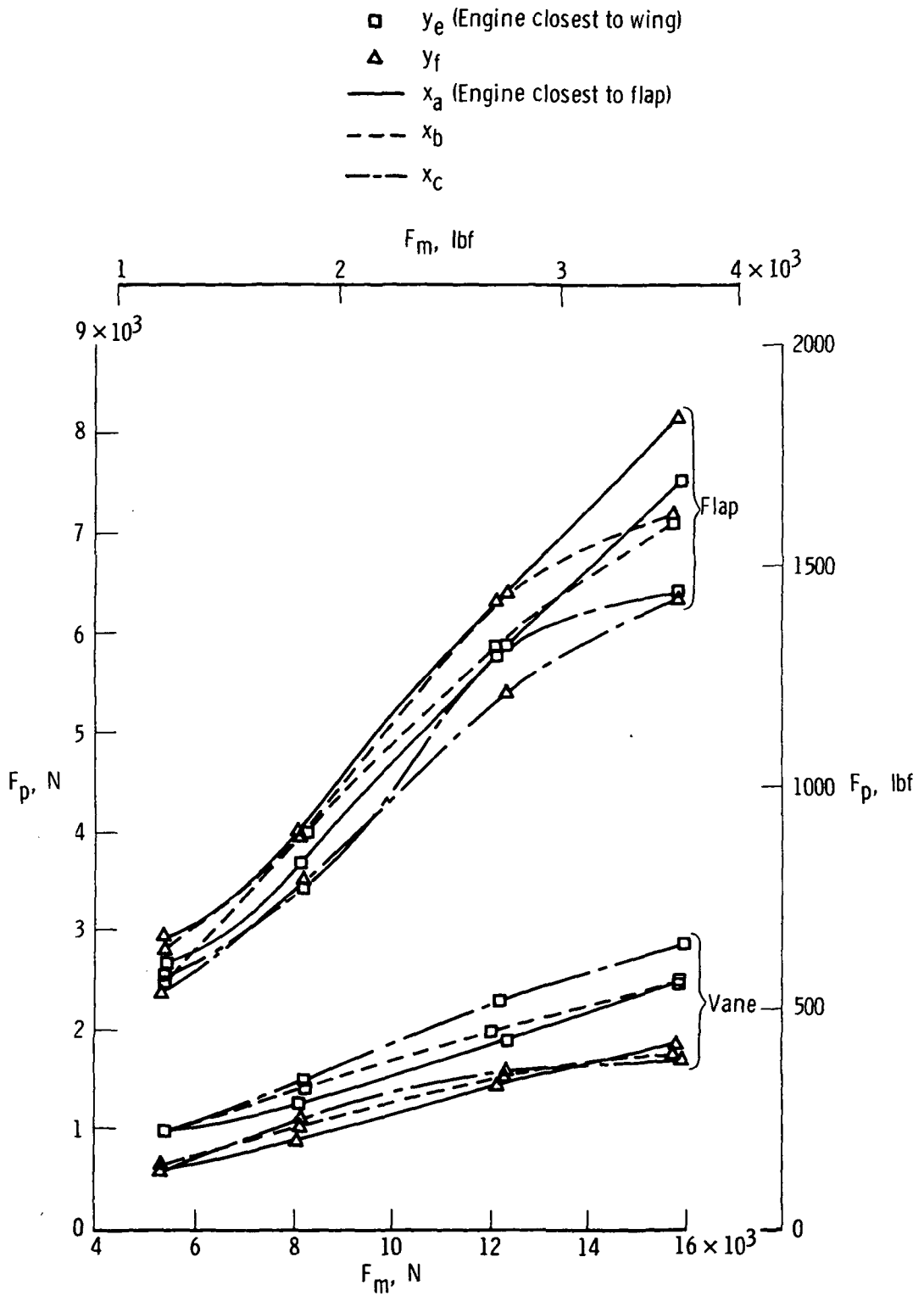

(b) Daisy nozzle, flaps deflected 60°.

Figure 11. Continued.

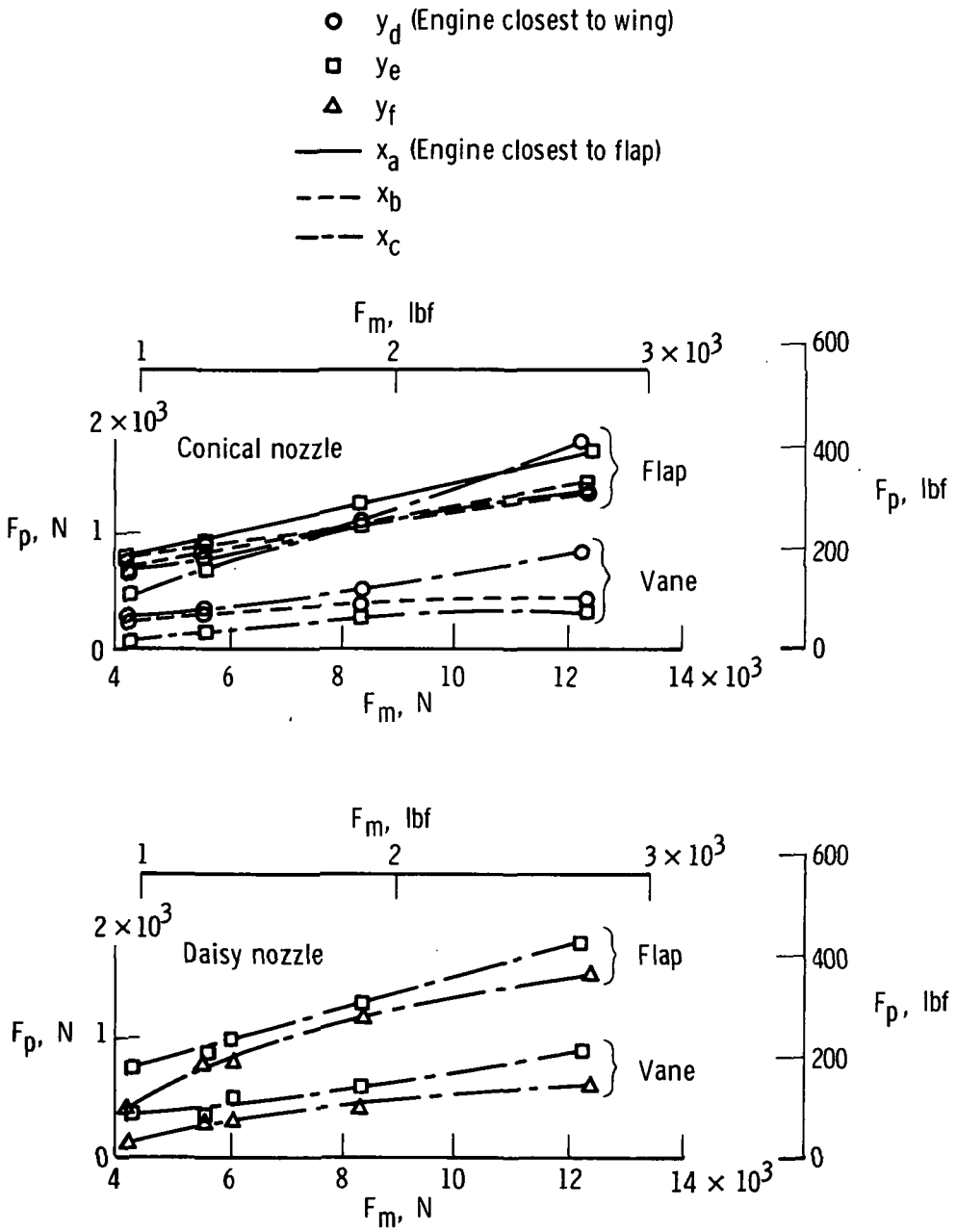

(c) Both nozzles, flaps deflected 35°.

Figure 11. Concluded.

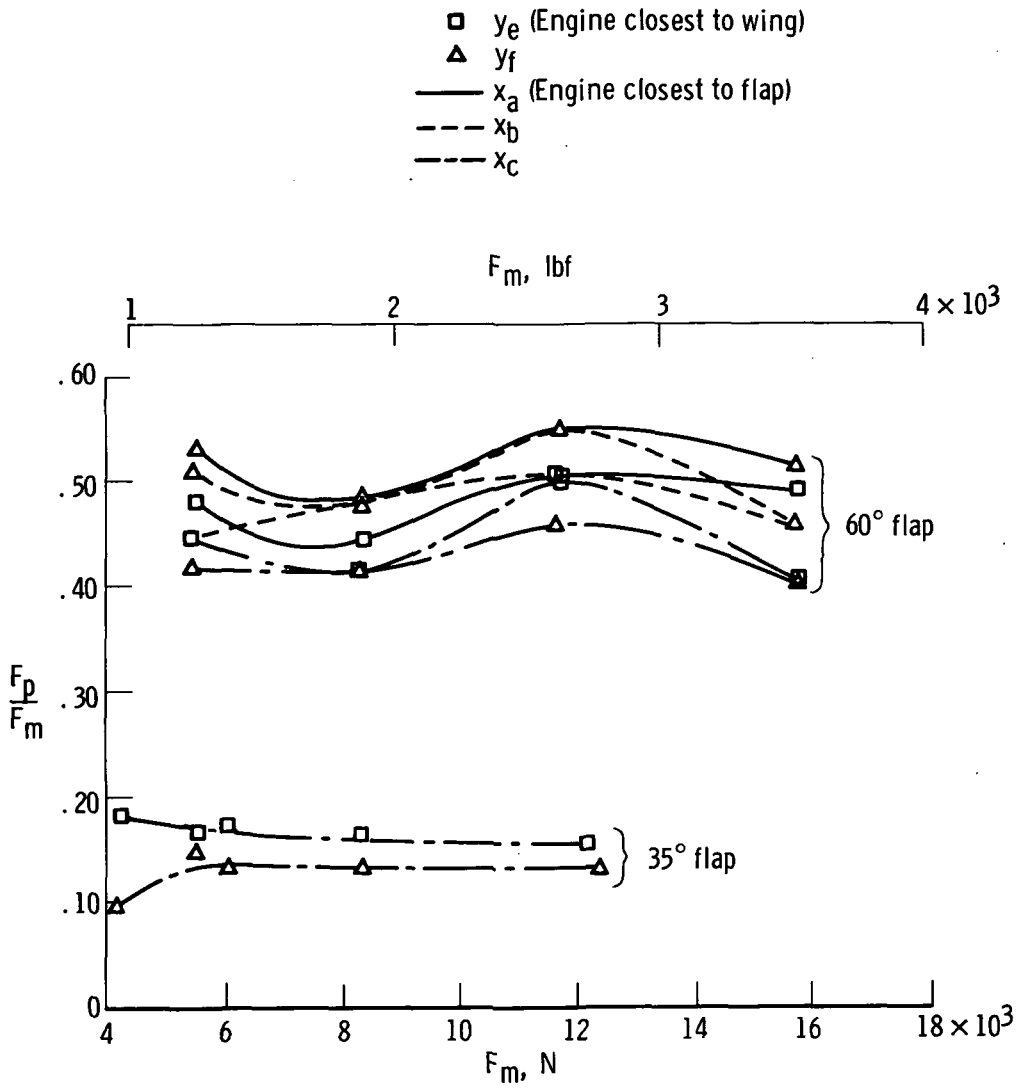

(a) Daisy nozzle.

Figure 12. Ratio of flap load to measured engine thrust over the test thrust range for several engine exhaust nozzle locations relative to the wing and flaps.

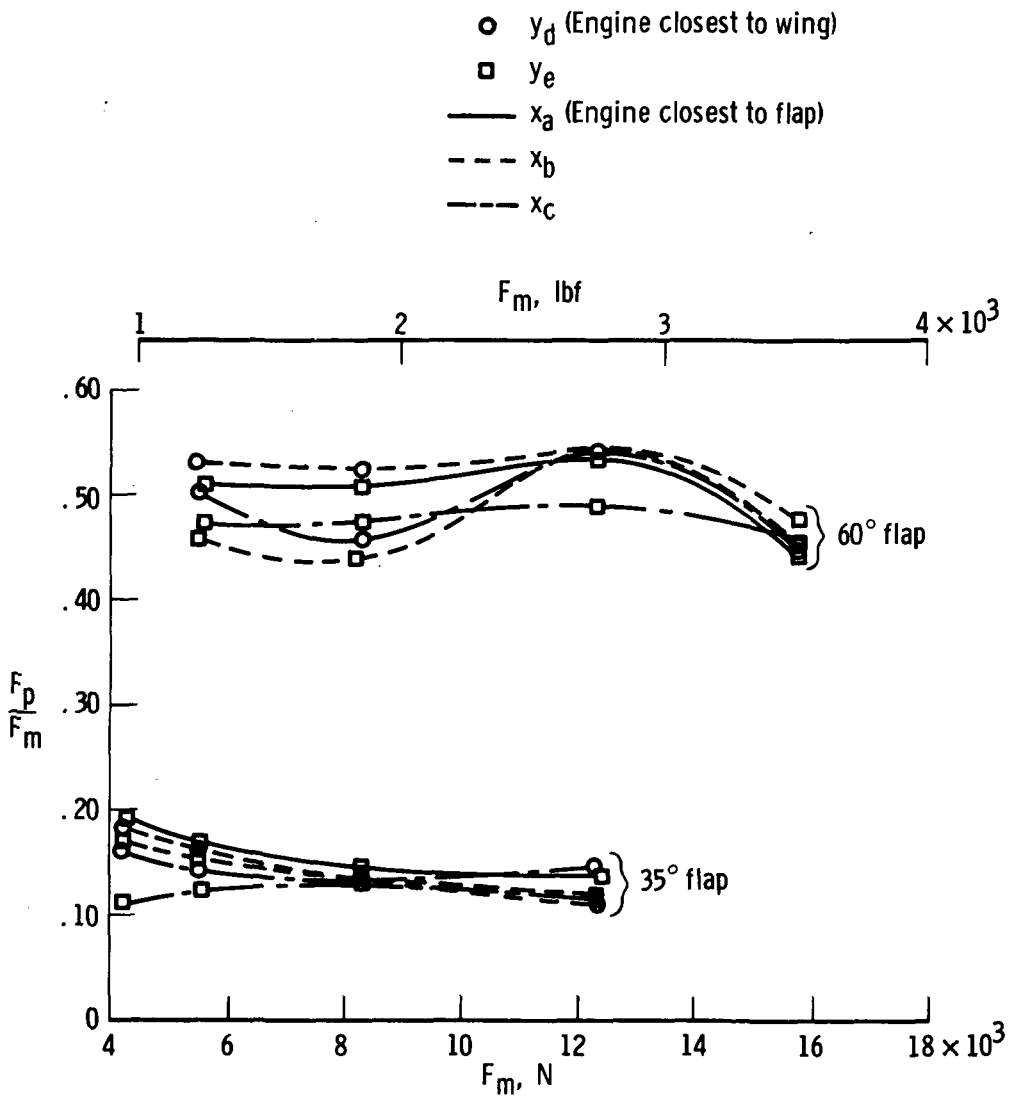

(b) Conical nozzle.

Figure 12. Concluded.

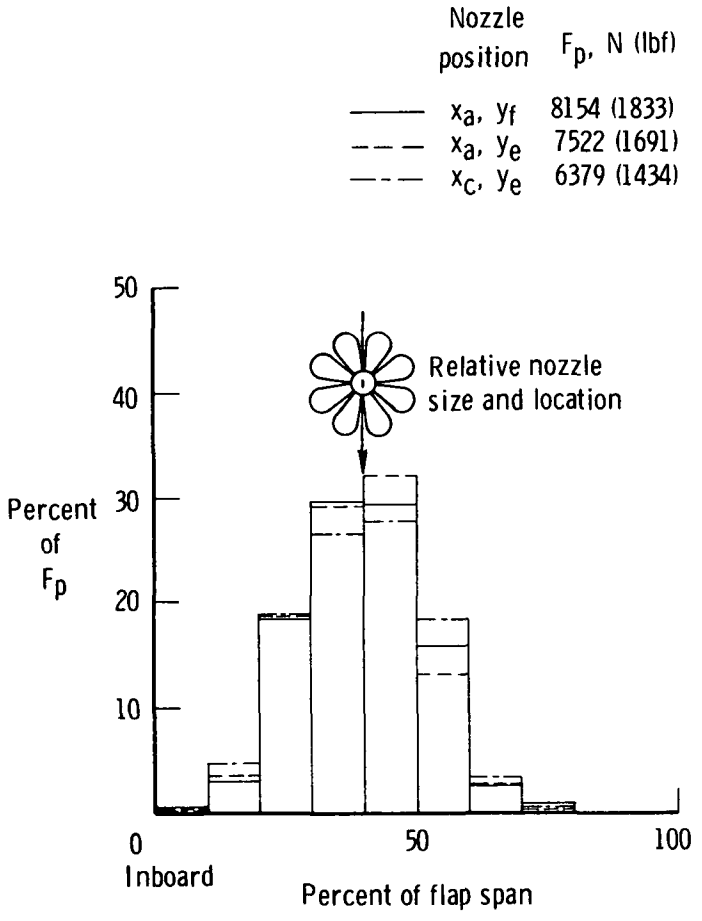

(a) Daisy nozzle.

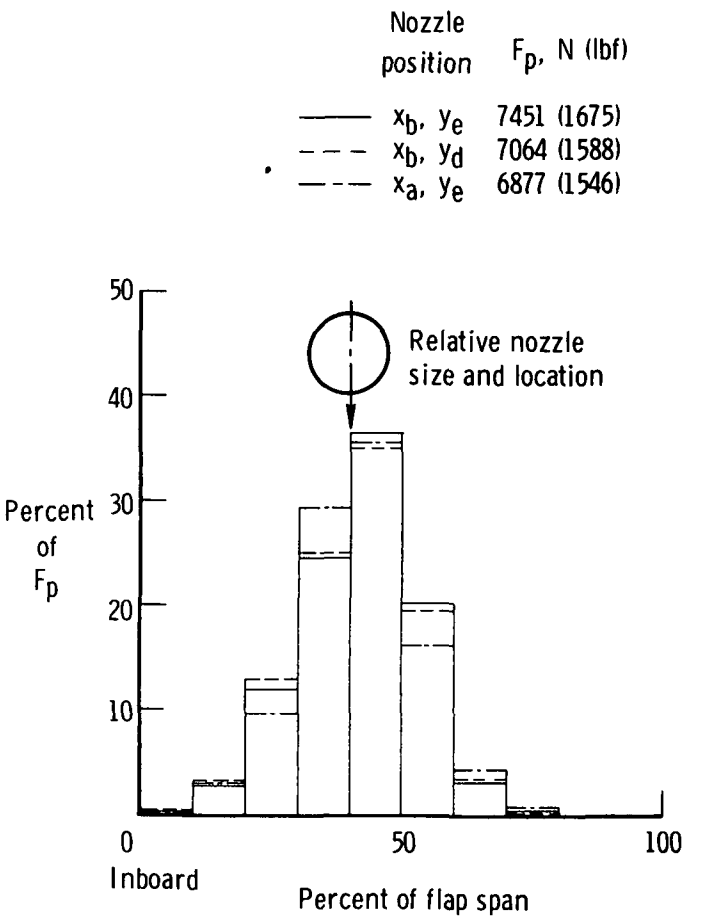

(b) Conical nozzle.

Figure 13. Distribution of the load over the span of the flap with the flaps deflected 60° for both nozzle configurations at three engine/wing positions. Test flap length, 3.81 m (150 in.); $\frac{N_f}{\sqrt{\theta}} \approx 8100$ rpm.

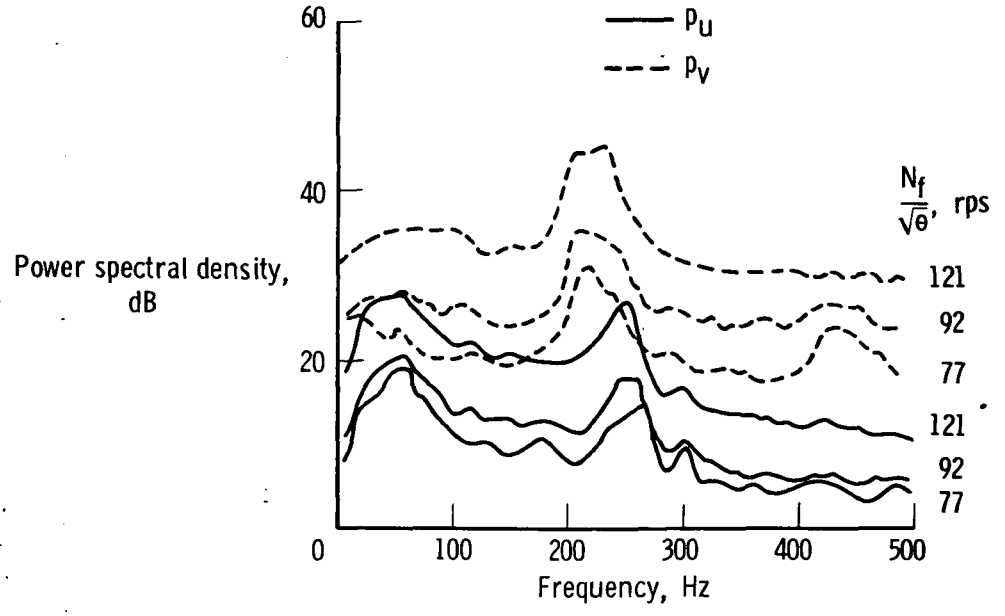

(a) Engine/wing position x_c, y_e.

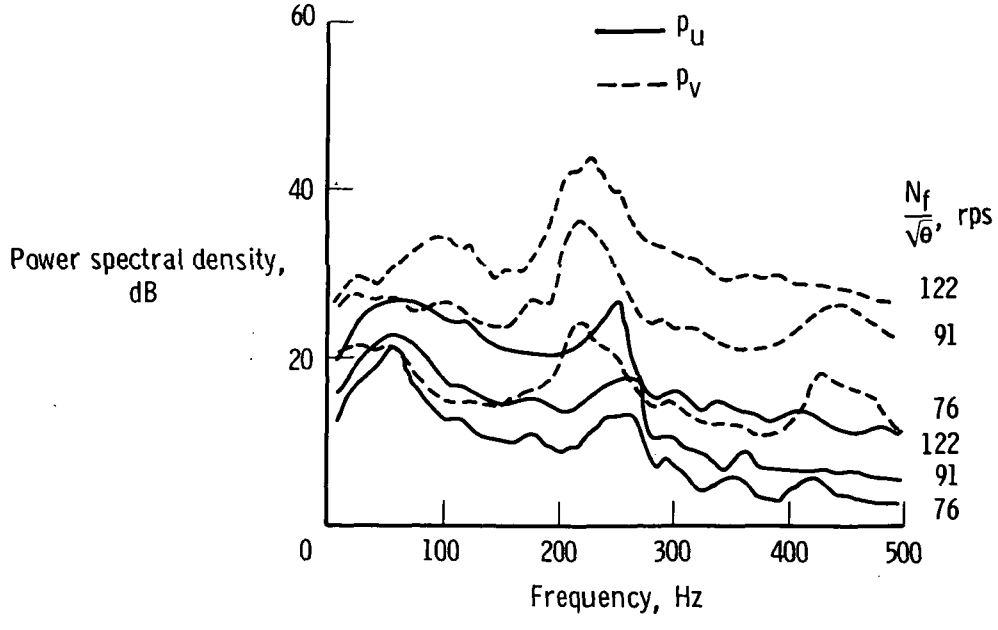

(b) Engine/wing position x_c, y_f.

Figure 14. Power spectral density plots of two static pressure measurements on the surface of the flaps which were deflected 35° during steady-state data runs with the daisy nozzle configuration.

NATIONAL AERONAUTICS AND SPACE ADMINISTRATION
WASHINGTON, D.C. 20546

OFFICIAL BUSINESS
PENALTY FOR PRIVATE USE $300

SPECIAL FOURTH-CLASS RATE
BOOK

POSTAGE AND FEES PAID
NATIONAL AERONAUTICS AND
SPACE ADMINISTRATION
451

U.S.MAIL

POSTMASTER: If Undeliverable (Section 158 Postal Manual) Do Not Return

"The aeronautical and space activities of the United States shall be conducted so as to contribute . . . to the expansion of human knowledge of phenomena in the atmosphere and space. The Administration shall provide for the widest practicable and appropriate dissemination of information concerning its activities and the results thereof."

—NATIONAL AERONAUTICS AND SPACE ACT OF 1958

NASA SCIENTIFIC AND TECHNICAL PUBLICATIONS

TECHNICAL REPORTS: Scientific and technical information considered important, complete, and a lasting contribution to existing knowledge.

TECHNICAL NOTES: Information less broad in scope but nevertheless of importance as a contribution to existing knowledge.

TECHNICAL MEMORANDUMS: Information receiving limited distribution because of preliminary data, security classification, or other reasons. Also includes conference proceedings with either limited or unlimited distribution.

CONTRACTOR REPORTS: Scientific and technical information generated under a NASA contract or grant and considered an important contribution to existing knowledge.

TECHNICAL TRANSLATIONS: Information published in a foreign language considered to merit NASA distribution in English.

SPECIAL PUBLICATIONS: Information derived from or of value to NASA activities. Publications include final reports of major projects, monographs, data compilations, handbooks, sourcebooks, and special bibliographies.

TECHNOLOGY UTILIZATION PUBLICATIONS: Information on technology used by NASA that may be of particular interest in commercial and other non-aerospace applications. Publications include Tech Briefs, Technology Utilization Reports and Technology Surveys.

Details on the availability of these publications may be obtained from:

SCIENTIFIC AND TECHNICAL INFORMATION OFFICE

NATIONAL AERONAUTICS AND SPACE ADMINISTRATION

Washington, D.C. 20546